

Degradation mechanism of a Golgi-retained distal
tubular acidosis mutant of the kidney Anion
Exchanger
1 in renal cells

by

Mattia Berrini

A thesis submitted in partial fulfillment of the requirements for the
degree of

Master of Science

In

Cell Biology

Department of Physiology

University of Alberta

© Mattia Berrini, 2014

Abstract

Distal renal tubular acidosis (dRTA) is a renal disease caused in some cases by mutations in the SLC4A1 gene encoding the kidney anion exchanger 1 (kAE1). Both recessive and dominant mutations result in mis-trafficking of proteins, preventing them from reaching the basolateral membrane of renal epithelial cells where their function is needed. kAE1 G701D is a functional, Golgi-retained dRTA mutant. The purpose of this thesis is to understand the degradation pathways of kAE1 G701D. We show that this mutant is poly-ubiquitylated and degraded by both lysosomal and proteasomal pathways. We provide evidence that the Nedd4 family interacting protein 1 (Ndfip1) interacts with kAE1 G701D, suggesting a possible role of Ndfip1 in the ubiquitylation process of this mutant. Also, we show that this mutant reaches temporarily the cell surface where it is endocytosed and degraded by the lysosomes via a peripheral quality-control machinery dependent mechanism. Furthermore we show that the function of kAE1 G701D is rescued at the cell surface upon inhibition of the lysosome and incubation with the chemical chaperone dimethyl sulfoxide (DMSO).

This study suggests that modulating the peripheral quality-control machinery may provide novel therapeutic strategies for the treatment of dRTA patients.

Table of Contents

Chapter 1. General introduction.....	1
1.1 Nephron and intercalated cells.....	2
1.1.1 Kidney - Main features.....	2
1.1.2 Nephron.....	2
1.1.3 Principal Cells.....	4
1.1.4 Intercalated Cells.....	6
1.2 Location and function of Anion Exchanger 1.....	6
1.2.1 eAE1.....	7
1.2.2 kAE1.....	9
1.2.3 AE1 Trafficking.....	11
1.3 AE1 associated diseases and conditions.....	19
1.3.1 dRTA.....	19
1.3.2 Hereditary spherocytosis.....	24
1.3.3 SAO.....	24
1.4 Aim of the present research.....	26
Chapter 2. Materials and Methods.....	27
2.1 Construction of kAE1 mutants.....	28
2.2 Cell lines.....	28
2.3 Transfections and viral infections.....	29
2.4 Lysate preparation and western blots.....	29
2.5 Immunoprecipitation.....	30
2.6 Immunocytochemistry.....	30
2.7 Imaging.....	31
2.8 Functional Assay.....	31
2.9 Statistical Analysis.....	32
Chapter 3. Results.....	33
3.1 Half-life of Golgi- and ER- retained kAE1 dRTA mutants.....	34
3.2 The Golgi-retained kAE1 G701D mutant is degraded by both the proteasome and lysosome.....	36

3.3 ER-retained mutant and Golgi-retained mutant are poly-ubiquitylated upon inhibition of degradation machineries.....	39
3.4 The Golgi-retained kAE1 G701D mutant transiently reaches the plasma membrane prior to degradation.....	42
3.5 The endocytosed kAE1 G701D mutant colocalizes with lysosome.....	43
3.6 Knocking down components of the peripheral quality-control machinery stabilizes rescued kAE1 G701D mutant.....	45
3.7 Inhibiting the lysosome restores the function of kAE1 G701D mutant..	49
3.8 Ndfip1 interacts with kAE1 G701D mutant.....	52
Chapter 4. Discussion.....	57
4.1 kAE1 G701D and C479W mutants are prematurely degraded.....	58
4.2 kAE1 G701D mutant is poly-ubiquitylated.....	59
4.3 kAE1 G701D transiently reaches the cell surface.....	60
4.4 Leupeptin treatment can improve the function of kAE1 G701D.....	62
4.5 Knocking down the peripheral quality-control machinery helps to stabilize kAE1 G701D.....	63
4.6 Ndfip1 interacts with kAE1 G701D.....	64
4.7 Final remarks.....	65
Chapter 5. Bibliography.....	67

List of tables

Table 1. Inheritance of characterized kAE1 mutations.....21

List of figures

Figure 1.1. Schematic representation of a nephron.....	3
Figure 1.2. Schematic representation of a Type A and Type B intercalated cell and of a Principal cell.....	5
Figure 1.3. Schematic representation of AE1.....	8
Figure 1.4. Schematic representation of the ubiquitylation pathway.....	12
Figure 1.5. Schematic representation of the protein trafficking and of the endosome-lysosome pathway.....	15
Figure 3.1. kAE1 mutants are prematurely degraded.....	35
Figure 3.2. Both the lysosome and proteasome participate in the degradation of the Golgi-retained and ER retained kAE1 mutants.....	37
Figure 3.3. Chloroquin inhibits lysosomal degradation of kAE1 G701D.....	38
Figure 3.4. kAE1 dRTA mutants are poly-ubiquitylated.....	40
Figure 3.5. kAE1 dRTA mutants are poly-ubiquitylated (RIPA buffer assay).....	41
Figure 3.6. kAE1 G701D mutant transiently reaches the plasma membrane.....	44
Figure 3.7. Endocytosed kAE1 G701D mutant partially co-localizes with lysosomal marker Lamp-1.....	46
Figure 3.8. Knocking-down components of the peripheral quality-control machinery stabilizes kAE1 G701D.....	48
Figure 3.9. Functional assay.....	51
Figure 3.10. kAE1 WT and G701D colocalize with Ndfip1.....	53
Figure 3.11. Ndfip1 interacts with kAE1.....	56

List of Abbreviations

AE	Anion Exchanger
BCECF-AM	2',7'-Bis(2-carboxyethyl)-5(6)-carboxyfluorescein-acetoxymethyl ester
CA	Carbonic Anhydrase
CHX	Cycloheximide
Cl ⁻	Chloride
CO ₂	Carbon Dioxide
DMSO	Dimethyl Sulfoxide
dRTA	distal Renal Tubular Acidosis
eAE1	erythroid Anion Exchanger 1
FBS	Fetal Bovine Serum
kAE1	kidney Anion Exchanger 1
E1	ubiquitin activating enzyme
E3	ubiquitin ligase
ER	Endoplasmic Reticulum
HA	Hemagglutinin
HCO ₃ ⁻	Bicarbonate
HEK	Human embryonic kidney
HRP	Horseradish Peroxidase
Hrs	Hepatocyte growth factor-regulated
HS	Hereditary Spherocytosis
MDCK	Madin Draby Canine Kidney
Ndfip	Nedd4 family interacting protein
NT	Non Targeted
SAO	Southeast Asian Ovalocytosis
STAM	Signal Transducing Adaptor Protein
Tsg	Tumor susceptibility gene
WT	Wild

Chapter 1. General Introduction

1.1 Nephron and intercalated cells

1.1.1 Kidney - Main features

Kidneys are paired retroperitoneal organs, located in the posterior part of the abdomen. The human kidney is approximately 12 cm in length, from 5 cm to 7.5 cm in width and about 3 cm in thickness (Glodny, Unterholzner et al. 2009).

Two distinct regions compose this organ: an outer one, the cortex, and an inner one, the medulla. The medulla is divided into 8 to 18 different conical masses, the renal pyramids. Each pyramid contains thousands of nephrons, tubular structures that represent the morphological and functional unit of the kidney. The base of each pyramid is positioned at the boundary between the cortex and the medulla. The pyramid tips converge in the calices where the small openings present on each tip form the area cribrosa. The calices converge, forming the renal pelvis, which represent the upper portion of the urinary tract (Glodny, Unterholzner et al. 2009).

1.1.2 Nephron

-Structure and anatomic description of the different portions

As mentioned before, the nephron is the morphological and functional unit of the kidney (Fig. 1). Each human kidney contains from 600.000 to more than one million of these units (Schreuder 2012). The essential components of the nephron include the Malpighian corpuscle, the proximal tubule, the thin limb, the distal tubule and the collecting duct.

Composed of a glomerulus and the Bowman's capsule, the Malpighian corpuscle is the nephron's initial filtering component. Fluids from blood in the glomerulus are filtered through the layer of podocytes, and the resulting filtrate is further processed along the nephron to form urine. The malpighian corpuscles are located in the cortex of the kidney. Where the proximal tubule becomes straight the nephron dives deeply into the kidney medulla where it turns back, ascending

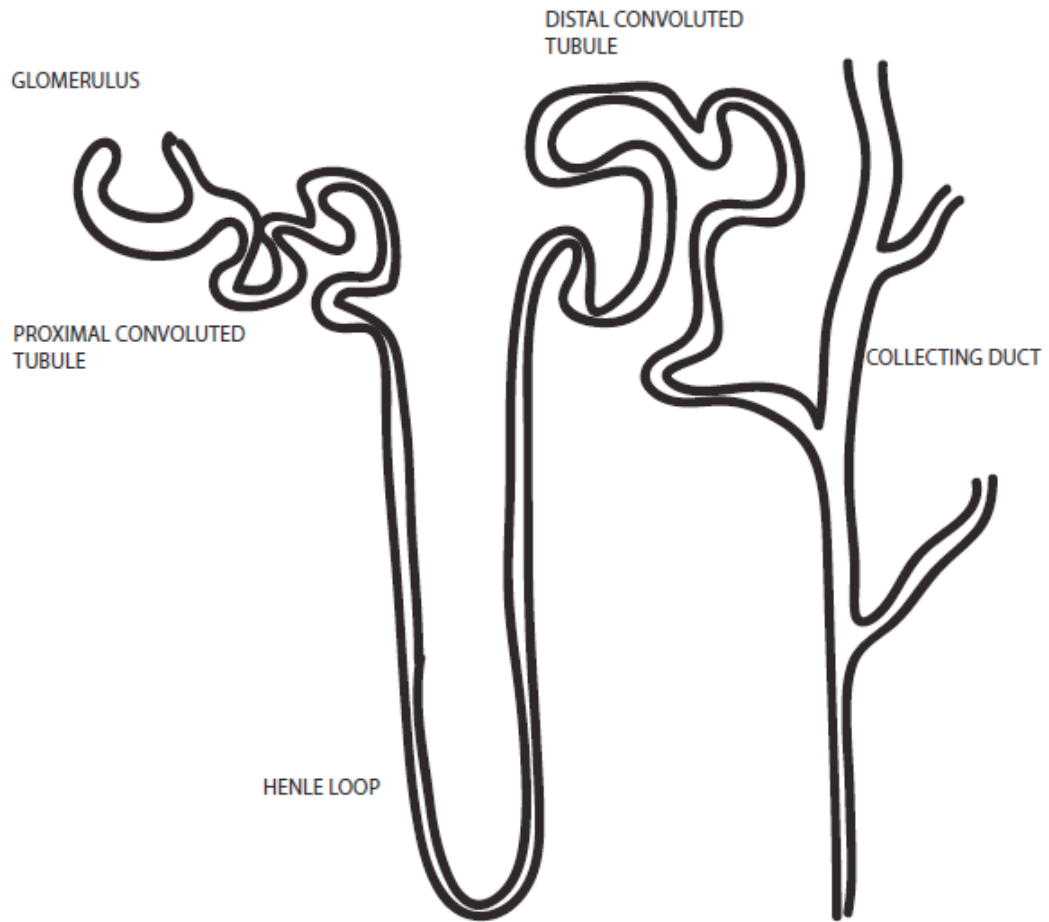


Figure 1.1 Schematic representation of a nephron

to the cortex again and thus forming the U-shaped loop of Henle (Schreuder 2012). Once back in the cortex, the fluid in the nephron enters the distal convoluted tubule before flowing in the collecting duct.

-Functionality and physiology of the nephron: ion exchanges

The main function of the nephron is to reabsorb and secrete various solutes such as ions, carbohydrates and amino acids. Properties of the cells found on the nephron epithelium change significantly along its length; thus, each segment of the nephron has highly specialized functions (Hou, Rajagopal et al. 2013). Approximately the 65% of filtered salt and water together with glucose and amino acids are reabsorbed from the proximal tubule to the peritubular capillaries (Glodny, Unterholzner et al. 2009, Hou, Rajagopal et al. 2013). In the loop of Henle the filtered salt is concentrated in to the surrounding tissue. The descending limb is permeable to water and impermeable to salt, thus, as the filtrate descends water gets out from the limb until the filtrate reaches the same tonicity of the surrounding tissue. The ascending limb is impermeable to water but it actively removes sodium from the filtrate making it hypotonic compared to the surrounding tissue (Hou, Rajagopal et al. 2013). Epithelial cells in the distal convoluted tubule and the collecting duct promote active transport of ions regulated by the endocrine system (Hou, Rajagopal et al. 2013). The epithelium of the collecting duct hosts principal cells and intercalated cells. The anion exchanger 1, which is the focus of this thesis is expressed in intercalated cells. However, to understand the physiology of this segment of the nephron, I need to describe the functions and characteristics of the two main cell types.

1.1.3 Principal cells

Principal cells are responsible for Na^+ reabsorption through the Epithelial Sodium Channel (ENaC) expressed at the apical membrane (Fig. 2) (Wang, Leroy et al. 2014). The expression of ENaC channel is regulated by aldosterone, which is released by the cortical component of the adrenal gland in case of low blood volume (hypovolemia) (Shibata, Rinehart et al. 2013). Na^+ ions are then extruded

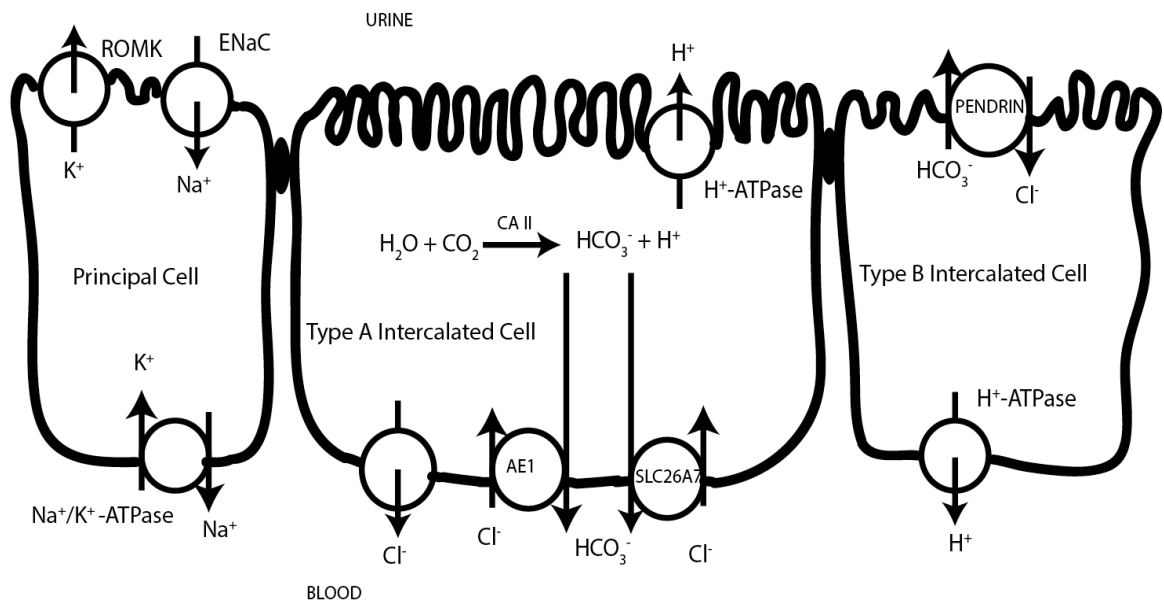


Figure 1.2. Schematic representation of a Type A and Type B intercalated cell and of a Principal cell. (ENaC: epithelial sodium channel, ROMK: renal outer medullary potassium).

through the basolateral membrane into the blood stream by a Na^+/K^+ ATPase. The same protein is responsible for the K^+ internalization from the blood into the cell. K^+ ions are then secreted into the urine via Renal Outer Medullary Potassium (ROMK) channels (Wang, Leroy et al. 2014).

1.1.4 Intercalated cells

The intercalated cells are present in the epithelium of the collecting duct of all mammalian kidney (Al-Awqati and Gao 2011). They exist in two forms: type A and type B (or α and β). Non-A, non-B intercalated cells have been localized as well in the cortical collecting duct and their main role is to absorb Cl^- and secrete HCO_3^- through the apical Na^+ -independent $\text{Cl}^-/\text{HCO}_3^-$ exchanger, pendrin (Wall 2005). In the type A intercalated cell the hydration reaction of CO_2 produces a proton and a HCO_3^- . Protons are secreted into the urine through a H^+ -ATPase present at the apical plasma membrane. HCO_3^- is moved to the blood stream through the kidney isoform of the anion exchanger 1 (AE1), the main topic of the present work, located at the basolateral membrane. The type B cell, reversely, secretes HCO_3^- into the duct lumen and protons into the blood (Al-Awqati and Gao 2011). In addition to different functions the two types show as well morphological differences: the type A intercalated cells show a more columnar shape with apical microvilli cytoplasmic area full of vesicles just underneath the apical membrane. Type B intercalated cells typically have a more eccentric nucleus, but does not show microvilli or vesicles (Bagnis, Marshansky et al. 2001). It has been proved that the two types of intercalated cells represent two different states of differentiation, where type B are less differentiated and are progenitors of type A (Vijayakumar, Takito et al. 1999).

1.2 Location and function of Anion Exchanger 1

In type A intercalated cells, the membrane protein Anion Exchanger 1 (AE1) is a chloride and bicarbonate exchanger, involved in maintaining acid-base

homeostasis in the human body (Duangtum, Junking et al. 2011). Encoded by the *SLC4A1* gene, AE1 is a dimeric membrane protein expressed both in erythrocytes (eAE1) and kidney type A intercalated cells (kAE1). In the human genome the *SLC4A1* gene is located on chromosome 17 with different promoters for the kidney and the red-blood cell isoforms (Barneaud-Rocca, Etchebest et al. 2013). At the molecular level, this protein is divided into two main structural domains: a cytoplasmic N-terminal domain (about 400 amino acids) and a membrane-spanning domain (about 450 amino acids) with a short C-terminal tail in the cytoplasm (Fig. 3). These two domains function independently from each other: the large cytoplasmic domain is involved in interactions with enzymes and structural proteins, while the membrane-spanning domain is responsible for the transport activity of the protein (Barneaud-Rocca, Etchebest et al. 2013).

The model represented in figure 3 shows the protein with 12 transmembrane domains but this number is still controversial. Bonar et al. have indeed developed a 13 transmembrane domains-model of AE1 (Bonar and Casey, 2008).

Few inhibitors of this protein have been identified. The best-characterized ones are the stilbenedisulfonates, which can compete with substrate anion for the binding site (Salhany 2001).

1.2.1 eAE1

The erythrocyte isoform of anion exchanger 1 (eAE1), also known as Band 3, is a major integral protein of the human erythrocyte membrane. It is a 911 amino acid glycoprotein with 13 transmembrane domains (Casey and Reithmeier 1998, Cheung, Li et al. 2005) that is responsible for the electroneutral exchange of bicarbonate for chloride (Pang, Bustos et al. 2008). Human AE1 has a monomeric molecular weight of 95 kDa and exists as a dimer and a tetramer in the red blood cell membrane (Casey et al., 1991). Walder et al. showed that mild proteolytic cleavage of this protein in erythrocyte membranes yields two functional domains (Walder, Chatterjee et al. 1984). The 52 kDa Carboxyl-terminal (C-terminal) transmembrane domain (Gly361–Val911) spans the membrane space 13 times and mediates the anion transport function (Casey and Reithmeier 1998). The 43

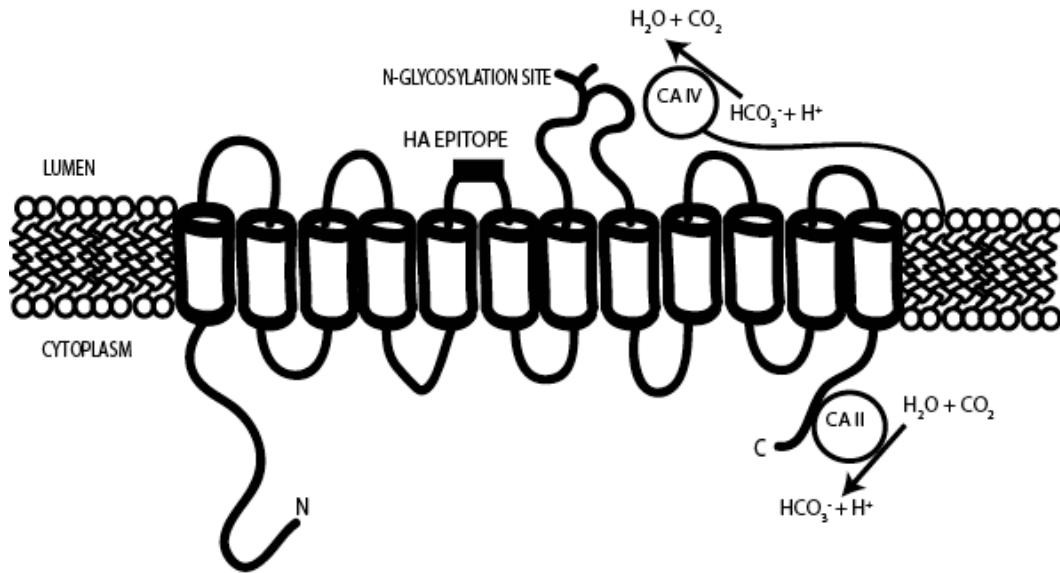


Figure 1.3. Schematic representation of AE1. CA II represents Carbonic Anhydrase II interacting with C terminal domain of kAE1. CA IV represents Carbonic Anhydrase IV bound to the plasma membrane through a glycosylphosphatidylinositol anchor.

kDa N-terminal cytosolic domain (from Met1 to Lys360) provides binding sites for various red cell cytoskeletal and cytosolic protein. The cytosolic domain of eAE1 acts as an anchoring site for ankyrin and protein 4.2, two proteins that are found in the erythrocyte membrane's cytoskeleton. So, because of its ability to interact with structural proteins, eAE1 seems to play an important role in maintaining the shape, stability, and flexibility of the red blood cell. eAE1 also binds and regulates the function of deoxyhemoglobin and various glycolytic enzymes such as glyceraldehyde-3-phosphate dehydrogenase, aldolase, and phosphofructokinase (Walder, Chatterjee et al. 1984, Pang, Bustos et al. 2008).

In addition, eAE1 interacts with several integral membrane proteins, including the chaperone-like protein glycophorin A, which provides further links between the membrane and the spectrin-based skeleton (Wu, Satchwell et al. 2011).

1.2.2 kAE1

The kidney isoform of anion exchanger 1 (kAE1) is a glycoprotein expressed at the basolateral membrane of type A intercalated cells in the collecting ducts of the kidney where it mediates electroneutral chloride/bicarbonate exchange (Williamson, Brown et al. 2008, Chu, King et al. 2013). Human kAE1 is a truncated form of erythroid AE1 missing the first 65 residues of the N-terminal cytosolic domain. Both N-terminal (residues 1-359) and C-terminal (residues 881-911) domains are located in the cytoplasm and are essential for basolateral trafficking of kAE1 (Williamson, Brown et al. 2008). The N-terminus of kAE1 interacts with the integrin-linked kinase (ILK), a protein that binds the cytoplasmic domains of β -integrins and cytoskeleton-associated proteins (Keskanokwong, Shandro et al. 2007). This interaction enhances kAE1 trafficking to the plasma membrane in human embryonic kidney (HEK293) cells (Keskanokwong, Shandro et al. 2007), but it seems that deletion of the majority of the ILK-interacting region in kAE1 had no effect on polarized trafficking of kAE1 in Madin–Darby canine kidney (MDCK) cells (Keskanokwong, Shandro et al.

2007). Toye et al. demonstrated that kAE1–ILK interaction is critical to maintain the basolateral membrane structure (Wu, Saleem et al. 2010).

The short cytosolic C-terminal is involved in physical interaction with carbonic anhydrase II (CAII), which catalyzes the production of bicarbonate and protons from water and CO₂ (Vince et al. 2000). The carboxyl-terminal interacts as well with both the adaptor protein 1 (AP1), which regulates processing of kAE1 to the cell surface (Almomani, King et al. 2012) and the glyceraldehyde 3-phosphate dehydrogenase (GAPDH), essential to kAE1 stability and involved in its proper trafficking to the cell surface (Su, Blake-Palmer et al. 2011).

kAE1 is organized in 12 transmembrane (TM) domains with an N-glycosylation site on the fourth extracellular loop (Vince et al. 2000). The fourth extracellular loop is responsible for the interaction with the Carbonic Anhydrase IV, which is anchored to the extracellular surface of the plasma membrane by a glycosylphosphatidyl-inositol anchor, thus reversibly hydrating CO₂ in the extracellular space (Sterling, Alvarez et al. 2002). Despite the importance of AE1 for acid-base homeostasis, not very much is known about its trafficking or regulation in the kidney. Animal studies suggested that Intercalated kidney cells increase AE1 levels at the basolateral membrane during chronic metabolic acidosis and reduce its levels during metabolic alkalosis events but the mechanism is still unknown (Sterling, Alvarez et al. 2002).

As described above, kAE1 is a bicarbonate-chloride exchanger (Huber, Asan et al. 1999). Type A intercalated cells express high amounts of cytosolic CA II, which allows the conversion of CO₂ and H₂O in HCO₃⁻ and H⁺. After this conversion, protons are extruded by the proton pump located on the apical membrane to the lumen of the collecting duct. HCO₃⁻ anions are moved into the blood stream by kAE1, expressed at the basolateral membrane in exchange with one anion chloride in the opposite direction. Intracellular chloride is then extruded through chloride channels on the basolateral membrane (Wagner, Devuyst et al. 2009). Thus, the correct targeting of kAE1 is essential for urinary acidification by the type A intercalated cells, where proton secretion by the apical H⁺-ATPase is coupled to the basolateral kAE1-mediated movement of bicarbonate out of the

cells (Wu, Satchwell et al. 2011).

1.2.3 AE1 Trafficking

- From the endoplasmic reticulum to the cell surface

Protein biosynthesis is mediated by the ribosomes that are located on the cytosolic face of the Endoplasmic Reticulum (ER) membrane. In the case of membrane proteins like AE1, as soon as the first part of the amino acidic sequence is assembled, the N-terminal α helix acts as an anchor sequence, directly binding the newly formed polypeptide chain to the ER membrane and initiating cotranslational insertion (Shao and Hegde 2011). The C-terminus of the chain keeps growing in the cytosol until the polypeptide is totally assembled.

Newly synthesized polypeptides undergo different modifications before they are targeted to their final destination (Figure 4).

The first modification is the formation of disulfide bonds. These covalent bonds are formed by the oxidative linkage of sulfhydryl groups on two cysteine residues in the same or different polypeptide chains. This kind of modification helps stabilize the tertiary and quaternary structure of the protein (Shao and Hegde 2011).

The second modification that occurs is the proper folding of the polypeptide. Several proteins present in the ER lumen, such as Calnexin and Calreticulin, Protein Disulfide Isomerase and the chaperone Hsc70, accelerate this process (Benham 2012). These proteins transiently bind to newly synthesized polypeptides and prevent them from misfolding. Calnexin is particularly critical at this step, interacting with the Asn-642 residue of AE1 (Popov and Reithmeier 1999). In the ER glycosylation with N-linked oligosaccharides occurs as well. N-linked oligosaccharides, which are bound to asparagine residues, contain a core of three mannose and two N-acetylglucosamine residues and have usually several branches (Aebi 2013). Popov and Reithmeier found that Calnexin binding to AE1 is enhanced by the presence of N-linked oligosaccharides (Popov and Reithmeier 1999). At this step, AE1 is glycosylated in its High-Mannose form.

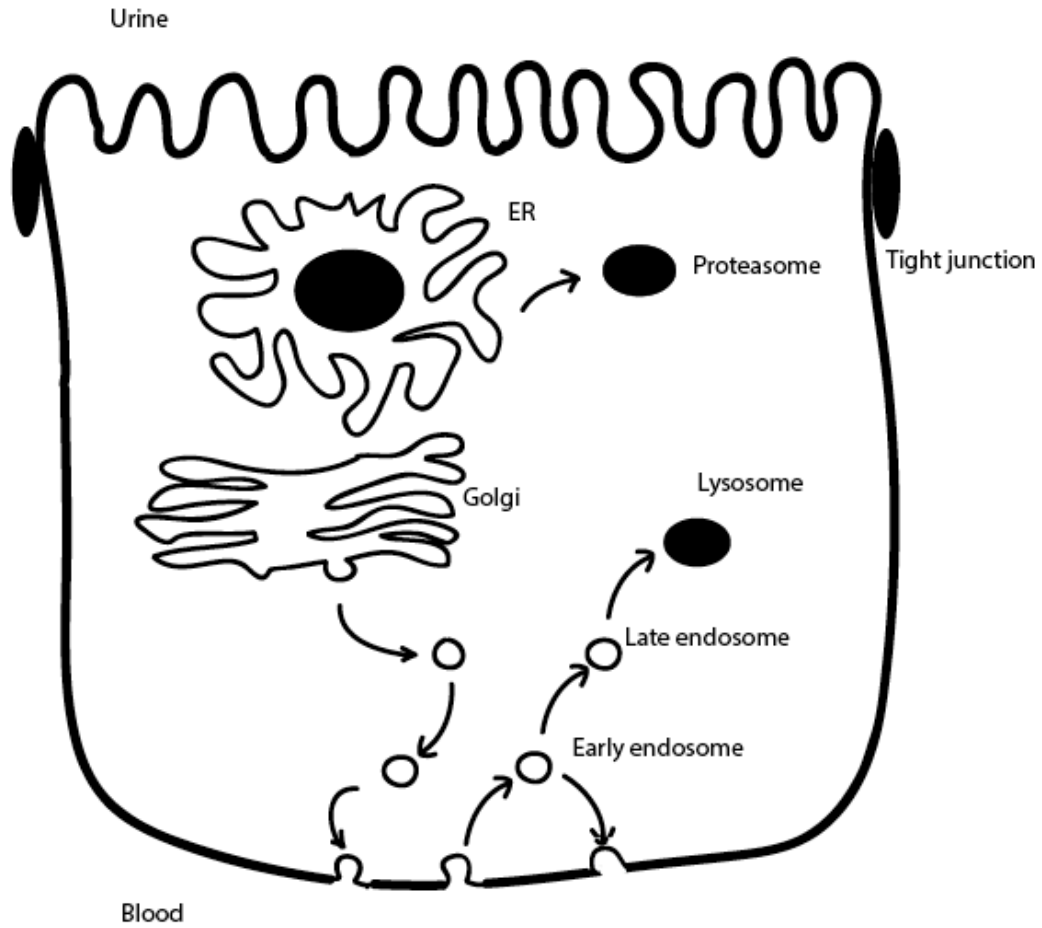


Fig. 1.4. Schematic representation of the protein trafficking and of the endosome-lysosome pathway. The position of the trafficking mutants of kAE1 G701D and C479W is displayed.

The third modification that typically happens in the ER is assembly of subunits into multimeric protein. At this step AE1 is assembled into a dimer (Zhang et al. 2000). Properly folded and assembled proteins are then loaded into vesicles formed by Coat Protein II (COPII) and transported to the Golgi complex (Hsu, Lee et al. 2009).

Proteins moved to the Golgi complex can undergo two more modifications. The first one is the glycosylation with O-linked oligosaccharides. O-linked oligosaccharides, which are bound to serine or threonine residues, are generally short, often containing only one to four sugar residues.

The second modification is represented by specific proteolytic cleavages. Many membrane proteins are synthesized as long, inactive precursors, called proproteins, that require further proteolytic processing, catalyzed by various proteases, to generate as final product the mature, active protein (Benham 2012). In the case of kAE1, the protein does not undergo any cleavage.

After all these processing, the final product is moved to its target location. Newly synthesized proteins are loaded into trafficking vesicles via interaction of specific recognition motifs within their cytosolic tail with adaptor proteins (AP) (Nakatsu et al. 2003). kAE1 interacts with the mu-1A and mu-1B subunits of the Adaptor Protein complex 1 (AP1) to be properly targeted to the cell surface (Almomani, King et al. 2012).

-Protein degradation

Mutant misfolded membrane proteins are usually degraded rapidly after their synthesis associated with the ER (Chang, Shaw et al. 2009). These proteins are transported from the ER into the cytosol where they are degraded by the ubiquitin-mediated proteolytic pathway (Jung and Grune 2013). To be targeted for degradation by the ubiquitin-mediated pathway, a protein must contain a structure that is recognized by an ubiquitinating enzyme complex. Different enzymes recognize different degradation signals in target proteins (Jung and Grune 2013). The ubiquitylation process involves the action of three families of enzymes. The E1 enzyme first activates ubiquitin by forming a covalent bond between the C-

terminus of ubiquitin and its own active site. Then ubiquitin passes to the E2 ubiquitin-conjugating enzyme. Finally the E3 ubiquitin-ligase promotes the transfer of ubiquitin onto the substrate (Kleiger and Mayor 2014). Nedd4 proteins, which belong to the E3 ubiquitin-protein ligase family, seem to play an important role in defining the substrate specificity of the ubiquitin system (Scheffner, Nuber et al. 1995). Ubiquitin ligases of the Nedd4 family are important for ubiquitylation processes downregulating the expression of cell surface proteins such as the epithelial sodium channel (ENaC) in the collecting duct of the kidneys (Kumar, Harvey et al. 1997). Ubiquitylation of proteins involves the action of the E1 ubiquitin-activating enzyme, E2 ubiquitin-conjugating enzymes and E3 ubiquitin-protein ligases. Nedd4 proteins, which belong to the E3 ubiquitin-protein ligase family, play an important role in defining the substrate specificity of the ubiquitin system (Scheffner, Nuber et al. 1995). Little is known about their adaptor, Nedd4 family-interacting protein1 (Ndfip1), beside the fact that it is implicated in the activation of Nedd4 itself and in its binding with the substrate protein (Goh, Low et al. 2013). Ndfip1 is an ubiquitin ligase adaptor, which in yeast is located in the Golgi, where it detects polar residues within transmembrane domains (Goh, Low et al. 2013). Ubiquitin-conjugating enzymes form a complex localized to the cytosolic face of the ER and recruit a degradation complex to the ER membrane where it can degrade misfolded proteins. The degradation machinery, then, proteolytically cleaves ubiquitin-tagged proteins in an ATP-dependent process, releasing intact ubiquitin molecules to the cytosol (Jung and Grune 2013) (Fig. 5).

In case of need to degrade a damaged or misfolded membrane protein already present at the cell surface, proteins are endocytosed and degraded via the lysosome degradation pathway. Lysosomal enzymes require acid pH to properly degrade peptides (Liu, Lu et al. 2008). The acidic environment inside lysosomes is provided by proton ATPases on the lysosomal membrane, and helps to denature the proteins.

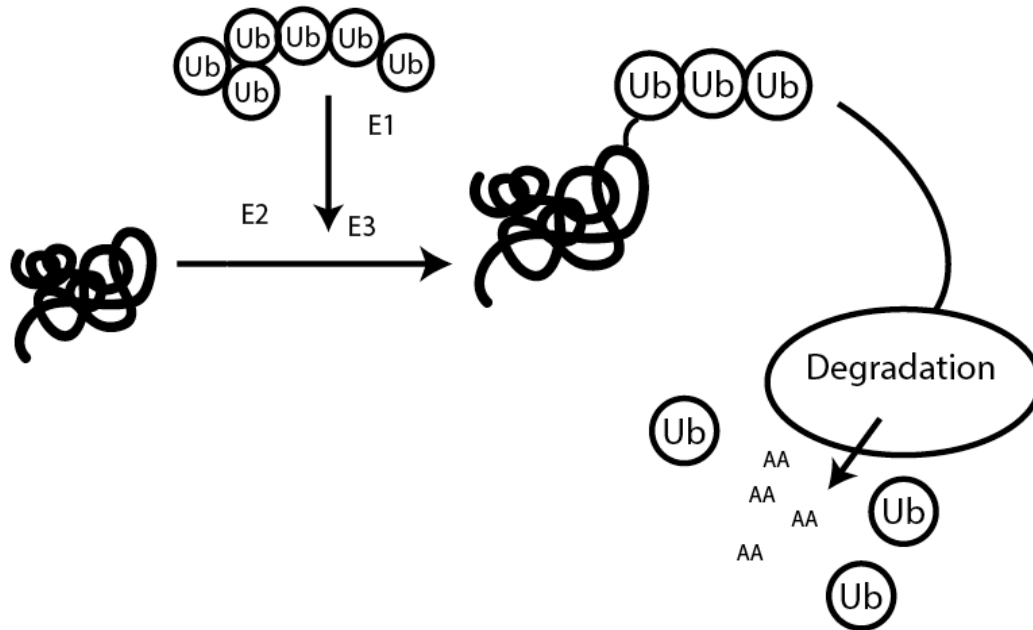


Fig. 1.5. Schematic representation of the ubiquitylation pathway. Enzymes belonging to classes E1 (ubiquitin-activating enzymes), E2 (ubiquitin-conjugating enzymes), and E3 (ubiquitin-ligase enzymes) add a variable number of ubiquitin molecules (Ub) to the peptide. The peptide is then recognized by the degradation machinery (either lysosome or proteasome) and degraded to single aminoacids (AA). Intact ubiquitin molecules are released in the cytosol.

-Protein recycling

Protein recycling indicates the processes involved in the re-insertion into the plasma membrane of endocytosed membrane proteins. The vesicles that transport proteins from one organelle to another represent a fundamental element of protein recycling. These vesicles typically arise from the membrane of an organelle (or from the plasma membrane) and fuse with the membrane of the target organelle. Thus, they are critical to the sorting of newly made proteins in the ER and of proteins internalized from the cell surface (Huotari and Helenius 2011). The process by which cells can internalize a molecule present on its surface or in the external environment goes under the name of endocytosis. Endocytosis is a crucial process, that enable cells to regulate the expression of surface components and to sample their environment (Bohdanowicz and Grinstein 2013). The vesicles that bud from the plasma membrane and internalize molecules present on the cell surface or inserted in the plasma membrane are called endosomes. Endosome budding is mediated by a protein coat formed of clathrin molecules that allows the membrane to invaginate (Royle 2006). Then, dynamin, a small GTPase, mediates the fission of the vesicle from the membrane (Henley, Cao et al. 1999). Based on the point of maturation of the vesicle, we can discriminate between early endosome and late endosome (Fig. 4).

Early endosomes provide the starting point for late endosome maturation, and they are recognized as the main sorting station in the endocytic pathway. The exact mechanism of formation of early endosomes is not entirely known, but the membrane is mainly derived from primary endocytic vesicles that fuse with each other (Huotari and Helenius 2011). After their internalization from the plasma membrane into early endosomes, molecules can either recycle to the plasma membrane via recycling endosomes, or be directed, via late endosomes, to the lysosomes for degradation (van Meel and Klumperman 2008) (Fig. 5).

Late endosomes are round or oval and have a diameter of 250-1000, nm are derived from the vacuolar domain of early endosomes (Huotari and Helenius 2011) and represent the last stage of endosomal maturation prior to fusing with

lysosomes. The maturation process involves exchange of membrane components, movement to the perinuclear area, a drop in luminal pH, acquisition of lysosomal components, and a change in morphology (Huotari and Helenius 2011). All these transformations are critical to definitely leave the recycling function of early endosomes and to allow the union of late endosomes with the lysosomes.

A specific family of GTP-binding proteins, the Rab proteins, participate in the control of vesicular and endosomal traffic in eukaryotic cells (Blumer, Rey et al. 2013). Rab proteins bind and hydrolyze GTP, thus regulating the rate of vesicle fusion. These molecules switch between active and inactive states by binding to GTP or GDP. Switching between these states is controlled by regulatory factors that activate (GDP/GTP exchange factors [GEFs]) or deactivate (GTPase activating proteins [GAPs]) the Rab protein (Blumer, Rey et al. 2013). The ability of Rabs to regulate membrane trafficking requires their physical connection to the endosomal membrane, which is allowed by the posttranslational modification of two cysteines at the structurally flexible C terminus of the GTPase with geranylgeranyl lipid portions. After inactivation via GAP-stimulated GTP hydrolysis, Rabs are solubilized by the molecular chaperone GDP dissociation inhibitor (GDI), which forms a cytosolic complex by interaction with the highly hydrophobic geranylgeranyl portions (Blumer, Rey et al. 2013). More than 70 different Rabs have been identified and many of them show a specificity of localization. In particular Rab 4 and Rab 14 show a specificity for early endosomes, while Rab 9 is mainly located in late endosomes (Stenmark and Olkkonen 2001). Rab 7, instead, participates to the maturation process of early endosomes into late endosomes (Huotari and Helenius 2011). Thus, Rabs provide the most important organelle identity marker and critical regulators in the endocytic pathway. Although each Rab seems to be specific for a particular cell component, most of them have not yet been properly investigated (Huotari and Helenius 2011).

-Mislocated proteins and associated diseases

The appropriate subcellular localization of proteins is critical because it provides the physiological environment appropriate for their function (Hung and Link

2011). A large percentage of the proteins synthesized by a cell have to be transported into or across at least one cellular membrane to reach their functional destination (Butler and Overall 2009). Improper protein localization can be caused not only by mutation of the protein itself, but as well by altered expression of cargo proteins or transport receptors or by deregulation of components of the trafficking machinery (Hung and Link 2011). No matter what the reason of mislocalization, mislocalization of misfolded proteins can have deleterious gain-of-function or dominant-negative effects in many diseases. Improperly localized proteins have been linked to many different human diseases such as Alzheimer's disease, kidney stones and cancer (Hung and Link 2011). Several hereditary genetic disorders have been linked to altered trafficking of misfolded G-protein-coupled receptors (GPCRs) like retinitis pigmentosa and nephrogenic diabetes insipidus (Conn, Ulloa-Aguirre et al. 2007). Consequently, targeting protein localization has been seen as a promising therapeutic strategy for treatment of several human diseases (Hung and Link 2011).

The final purpose of this research is to identify ways to rescue trafficking of functional kAE1 mutants. In this work we have focused on a Golgi-retained mutant that causes a human disease called distal renal tubular acidosis (see section 1.3.1 below). There are pharmaceutical agents that specifically target protein localization, but the spectrum of their use in clinical or preclinical development is still limited. From a functional point of view, these agents can be divided into two main classes: relocators that restore physiological protein localization and function, and mislocators that aim to intentionally cause protein mislocalization and thereby inhibit the function of disease-causing proteins (Hung and Link 2011). Many examples of relocators have been described in the recent past. For instance, the trafficking of the hepatocyte ER retained ATP-binding cassette 6 R1314W mutant was rescued by a 4-phenylbutyrate treatment (Le Saux, Fulop et al. 2011). The vasoactive intestinal peptide (VIP) can rescue the proper insertion of the mislocated CFTR F508del mutant in the plasma membrane (Rafferty, Alcolado et al. 2009). The corrector VX-809 stabilizes the first transmembrane domain of CFTR (Loo, Bartlett et al. 2013)

1.3 AE1 associated diseases and conditions

Twenty disease-causing mutants of kAE1 have been described so far (see Table 1). Some of them can be dominantly inherited, while others are recessive. Some are not functional while others show a normal functionality but are mistargeted to different cellular location than the basolateral membrane. The dominant mutants kAE1 R589H, R901X and S613F, which seem to have normal anion exchange function, show intracellular retention in the endoplasmic reticulum (Yenchitsomanus, Kittanakom et al. 2005). The R589 residue seems to be a mutational hotspot as many mutations have been identified in this position like kAE1 R589C and kAE1 R589S (Vasuvattakul 2010). The dominant mutants kAE1 R901X and G609R are mistargeted to the apical membrane (Yenchitsomanus, Kittanakom et al. 2005). The recessive mutant, kAE1 G701D, has a trafficking defect and is retained in the Golgi apparatus, while the recessive and mis-folded kAE1 S773P can only partially be delivered to the basolateral membrane (Yenchitsomanus, Kittanakom et al. 2005). Interestingly, some mutants that are mistargeted in kidney, as kAE1 G701D, have been found causing no disease in red blood cells, where the mutant is properly located at the cell surface because of the presence of the chaperone-like protein glycophorin A, thus showing that, despite its mistargeting, the mutant is still functional (Bruce, Wrong et al. 2000).

1.3.1 dRTA

Distal renal tubular acidosis (dRTA) is a rare disease that results from the impaired secretion of hydrogen ions from the distal nephron, causing metabolic acidosis, associated with kidney calcification (called nephrocalcinosis), low K^+ level in the blood (hypokalaemia) and metabolic bone disease (Bruce, Wrong et al. 2000). The cause is the impaired proton secretion by Type-A intercalated cells

of the renal collecting duct. In these cells, protons to be secreted are derived from the Carbonic Anhydrase II-catalyzed reaction of hydration of CO₂ to carbonic acid (Fig. 2), which dissociates to form bicarbonate and protons (Wrong, Bruce et al. 2002, Batlle and Haque 2012). Protons are then secreted through the proton pump located at the apical membrane while the bicarbonate generated by this process reaches the blood stream through the action of AE1 (Batlle and Haque 2012). Thus, a loss of AE1 function leads to accumulation of bicarbonate inside the cell. Consequently, this leads to a reduction in the dissociation of carbonic acid and reduced amount of protons for secretion into the tubular lumen and bicarbonate ions to be secreted in the blood (Wrong, Bruce et al. 2002). Several AE1 mutations can cause dRTA (Yenchitsomanus, Kittanakom et al. 2005), but the same disease can be caused as well by mutations on other genes that participate in the process described above. For instance mutations on the Carbonic Anhydrase II – encoding gene or on the gene encoding for the apical proton pump (Fry and Karet 2007, Batlle and Haque 2012). Furthermore, renal tubular acidosis can be frequently acquired due to use of drug used to treat autoimmune disease or to use of cyclosporine after kidney transplantation (Golembiewska and Ciechanowski 2012).

Table 1. Inheritance of characterized kAE1 mutations (Chu et al., 2012)

kAE1 mutation	Inheritance	Localization in MDCK cells	References
R589H	Dominant	ER	(Toye, Banting et al. 2004)
R589C	Dominant	ER	(Bruce, Wrong et al. 2000)
R589S	Dominant	ER	(Toye, Banting et al. 2004)
G609R	Dominant	Cell surface	(Yenchitsomanus, Kittanakom et al. 2005)
S613F	Dominant	ER	(Toye, Banting et al. 2004)
S667F	Dominant	ER	(Yenchitsomanus, Kittanakom et al. 2005)
A858D	Dominant	Cell surface	(Ungsupravate, Sawasdee et al. 2010)
A888LX	Dominant	Unknown	
R901X	Dominant	ER/Endosomes	(Toye, Banting et al. 2004)
D905Glyfs15	Dominant	Unknown	(Zhang, Liu et al. 2012)
D905dup	Dominant	Unknown	(Zhang, Liu et al. 2012)
M909T	Dominant	Cells surface	(Fry, Su et al. 2012)
C479W	Recessive	ER	(Chu, King et al. 2013)
V488M	Recessive	ER	(Cordat 2006)
G494S	Recessive	Unknown	(Zhang, Liu et al. 2012)
E522K	Recessive	Cell surface	(Chang, Shaw et al. 2009)
R602H	Recessive	Cell surface	(Kittanakom, Cordat et al. 2008)
G701D	Recessive	Golgi	(Chu, King et al. 2013)
S773P	Recessive	Cell surface	(Yenchitsomanus, Kittanakom et al. 2005)
ΔV850	Recessive	ER	(Kittanakom, Cordat et al. 2008)

-Effects, symptoms, pathology and treatments

dRTA represents a failure of the Type-A intercalated cells to acidify the urine. In its inherited form has three variants: autosomal dominant and autosomal recessive with or without deafness (Fry and Karet 2007). In the clinic, acquired forms predominate, most often as a result of autoimmune disease, other systemic disorders, or drugs (Fry and Karet 2007, Golembiewska and Ciechanowski 2012). Patients with dRTA are often growth-retarded because of chronic metabolic acidosis (Batlle and Haque 2012). Associated features are nephrocalcinosis, formation of kidney stones (nephrolithiasis), high concentration of calcium in the urine (hypercalciuria) and low concentration of citrate in the urine (hypocitraturia). The hypercalciuria is multifactorial, probably due to a combination of increased calcium release from bone, acidosis-induced downregulation of renal Ca^{2+} transport proteins, and increased distal sodium delivery (Fry and Karet 2007). These factors, together with the high urine pH, favor abnormal renal calcium deposition as nephrocalcinosis and renal stones, both of which may result in renal failure in the long term (Fry and Karet 2007). Rickets and osteomalacia (softening of the bones caused by defective bone mineralization) can develop in both dominant and recessive forms, although dominant disease typically presents more mildly in adolescence or adulthood, and recessive in infancy/early childhood (Fry and Karet 2007). Other extrarenal manifestations depend on the gene mutated and the type of mutation. Hemolytic anemia may be seen in some types of hereditary RTA associated with AE1 mutations, whereas deafness is an important feature in some H^+ -ATPase mutations (Batlle and Haque 2012).

Norgett et al. described a good animal model for H^+ -ATPase-caused dRTA: a knockout mouse (*Atp6v0a4*^{-/-}), which lacks the A4 subunit of the H^+ -ATPase (Norgett, Golder et al. 2012). Using β -galactosidase as a reporter for the null gene, developmental A4 expression was detected in developing bone, nose, eye, and skin, in addition to that expected in kidney and inner ear. By the time of weaning, *Atp6v0a4*^{-/-} mice demonstrated severe metabolic acidosis,

hypokalemia, and early nephrocalcinosis. Null mice were hypocitraturic, but hypercalciuria was absent. They died rapidly unless provided with alkaline diet.

Stehberger et al. described a mouse model that lacks AE1 (*slc4a1*^{-/-}) (Stehberger, Shmukler et al. 2007). This animal exhibited dRTA characterized by spontaneous hyperchloremic metabolic acidosis with low net acid excretion and, inappropriately, alkaline urine without bicarbonaturia. Differently, mice that were heterozygous for the AE1-deficient allele had no apparent defect. Thus, the *slc4a1*^{-/-} mouse has been the first genetic model of complete dRTA and demonstrates that the AE1 exchanger is required for maintenance of normal acid-base homeostasis by distal renal regeneration of bicarbonate in the mouse as well as in humans (Stehberger, Shmukler et al. 2007).

Diagnosis of classic dRTA is based on the finding of a high urine pH in the setting of a systemic metabolic acidosis. The systemic pH may be fully compensated in individuals with “incomplete” dRTA, in which case a failure of urinary acidification should be demonstrated pharmacologically. This is achieved through an oral ammonium-loading test, or a combination of furosemide/fluorocortisones has been proposed as an alternative (Unwin, Shirley et al. 2002). Moderate doses of oral alkali (1–3 mM a day of bicarbonate) are sufficient to reverse the metabolic acidosis and normalize bone growth but generate kidney stones (Fry and Karet 2007). However, even more important is the proper supplementation of potassium, as the correction of acidosis can enhance hypokalemia. This is because, providing exogenous bicarbonate to the blood, AE1 activity slows down thus reducing the intracellular Cl⁻ concentration and thus reducing available substrate for the Cl⁻/K⁺ cotransporter, responsible for moving K⁺ from the cell to the blood stream (Fry and Karet 2007). The preferred form of potassium administration is potassium citrate because of its alkalizing effect and protection against hypocitraturia (Golembiewska and Ciechanowski 2012). Fludrocortisone therapy may be useful, in combination with a loop diuretic (Golembiewska and Ciechanowski 2012).

As AE1 is also expressed in red blood cells, mutations in the SLC4A1 gene can also result in hematological problems, as discussed in the following sections.

1.3.2 Hereditary spherocytosis

Hereditary spherocytosis is one the most common form of anaemia, involving about 1 out of 5,000 people in the Caucasian population (Barcellini, Bianchi et al. 2011). This condition can result from a deficiency or a dysfunction of the erythroid form of AE1 but as well of ankyrin, spectrin and/or protein 4.2 (Barcellini, Bianchi et al. 2011, Wu, Satchwell et al. 2011). As these proteins connect AE1 in the plasma membrane to the cytoskeleton, the disease results in spheroid, fragile cells, that are usually rapidly degraded by the spleen. This results in a hyperactivity of the spleen that can easily lead to splenomegaly (abnormal growth of the spleen) (Barcellini, Bianchi et al. 2011).

1.3.3 SAO

Southeast Asian Ovalocytosis (SAO) is a red-cell abnormality common in the southeastern region of Asia, particularly in Malaysia and Papua New Guinea, where it affects up to 40% of the population in some coastal areas (Bruce, Wrong et al. 2000). The condition results from the heterozygous presence of a nine amino-acid deletion (400-408) in eAE1. This mutation is always accompanied by substitution of lysine 56 by glutamic acid (K56E), the asymptomatic “Memphis” polymorphism that is common in the general healthy population (Wrong, Bruce et al. 2002). eAE1 SAO is unable to transport anions and SAO red blood cells have an oval shape and an increased rigidity due to a stronger bond between eAE1 and ankyrin (Bruce, Wrong et al. 2000, Wrong, Bruce et al. 2002).

Among the other abnormalities that SAO erythrocytes show, there is a reduction in cellular sensitivity to osmotic pressure and a partial intracellular depletion of ATP (Wrong, Bruce et al. 2002). At the organism level, instead, one of the most remarkable effects is resistance to infection by the malaria pathogen *Plasmodium falciparum* (Wrong, Bruce et al. 2002, Rosanas-Urgell, Lin et al. 2012). AE1 aggregates normally present at the red-cell surface act as receptors for the parasite. The reason behind the plasmodium-resistance of the SAO erythrocyte is that the increased rigidity of the membrane reduces the capacity of AE1 protein

to cluster together, thus making it more difficult for the parasite to properly enter in the cell (Mohandas, Lie-Injo et al. 1984, Cortes, Benet et al. 2004).

- Correlations with dRTA

There have been several reports of an association between dRTA and SAO (Bruce, Wrong et al. 2000, Wrong, Bruce et al. 2002, Vasuvattakul 2010), but rarely the same mutation causes both diseases. The SAO deletion itself (deletion of residues 400-408) does not result in dRTA (Vasuvattakul 2010) but the compound heterozygotes of many dRTA mutations with SAO all had dRTA (Bruce, Wrong et al. 2000). Bruce et al. hypothesized that dRTA might arise by a different mechanism for each mutation.

On the other hand, we have many examples of a mutation leading to dRTA but resulting in no SAO: one of them, G701D AE1, indeed, is mistargeted to the Golgi apparatus in Type A intercalated kidney cells but properly located at the cell surface in red-blood cells (Vasuvattakul 2010). This is due to the fact that G701D AE1 requires glycophorin A, a protein expressed in erythrocytes but not in kidney cells to be targeted to the cell surface (Bruce, Wrong et al. 2000). Co-expression of kAE1 and kAE1 SAO with the dRTA mutants (G701D, Δ V850, R602H, and A858D) was also studied in polarized epithelial MDCK cells (Kittanakom, Cordat et al. 2008). The results showed that decreased cell-surface expression of the dRTA mutants as a result of the interaction with kAE1 SAO would account for the impaired expression of functional kAE1 at the basolateral membrane of type A intercalated cells. This results in dRTA in compound heterozygous patients. Moreover, red-cells and *Xenopus* oocyte expression studies showed that Δ V850 and A858D mutant have greatly decreased anion transport ability when present as compound heterozygotes, for instance as Δ V850/SAO or A858D/SAO (Bruce, Wrong et al. 2000).

1.4 Aim of the present research

In a paper published in 2013 we showed that 16 hours of treatment with 1% dimethyl sulfoxide can partially rescue trafficking of the dRTA Golgi retained kAE1 G701D mutant to the surface of MDCK cells (Chu, King et al. 2013). Nevertheless, this treatment has not been able to rescue the function of this mutant to the same level as the wild type (WT). This suggested the hypothesis that this mutant might be rapidly internalized and degraded. The interest about the kAE1 G701D mutant rises from the fact that the erythrocyte isoform of this mutant is properly inserted and functional in the plasma membrane of red blood cells (Bruce et al. 2000). This is because red blood cells express the chaperone Glycophorin A that allows the proper trafficking of eAE1 G701D to the cell surface (Bruce et al. 2000).

Other mistargeted mutants, like kAE1 C479W, have been shown to be non-functional, when expressed in *Xenopus* oocytes (Chu, Woods et al. 2010). Furthermore, the degradation mechanisms of a Golgi-retained mutant in mammalian cells are still unclear (Bruce et al. 2000).

This thesis therefore aimed at obtaining a better understanding of the degradation pathways of the dRTA mutant kAE1 G701D in order to identify a treatment eventually leading to a complete rescue of the mutant's functionality. A better understanding of these degradation mechanisms will also provide novel information on degradation pathways of Golgi retained proteins in mammalian cells, a pathway poorly characterized to date.

Thus, in this research we have been focusing on kAE1 G701D mutants, using the WT as positive control and the non-functional, ER retained mutant C479W as negative control.

Chapter 2. Materials and Methods

2.1 Construction of kAE1 mutants

Human kAE1 cDNA encoding for kAE1 WT, G701D and C479W, containing a hemagglutinin (HA) epitope encoding sequence expressed on the third extracellular loop, have been cloned into the viral vector pFB-Neo (Stratagene) to transfect MDCK cells.

Human kAE1 cDNA encoding for kAE1 WT, G701D and C479W, containing a hemagglutinin (HA) epitope encoding sequence, have been cloned into the vector pcDNA3 to transiently transfect LLC-PK1 and HeLa cells.

Human cDNA encoding for Ndfip1, containing a Flag epitope encoding sequence, have been cloned into the vector pcDNA3 to transiently transfect LLC-PK1 cells.

Human cDNA encoding the lysosomal marker Lamp-1 fused to Venus fluorescent protein have been cloned into the vector pcDNA3 to transiently transfect MDCK cells.

2.2 Cell lines

Madin-Darby canine kidney cells (MDCK), porcine kidney cells LLC-PK1 and human embryonic kidney (HEK 293), obtained from the American Type Culture Collection (ATCC, Manassas, USA) were grown in DMEM F-12 supplemented with 10% fetal bovine serum (FBS), 0.5% penicillin and 0.5% streptomycin at 37°C under 5% CO₂.

Ts20 cells were maintained in DMEM-F12, supplemented with 10% foetal bovine serum (FBS), 0.5% penicillin and 0.5% streptomycin at 30°C under 5% CO₂. Inactivation of the ubiquitin-activating enzyme E1 resulted from a 2 h incubation of the cells at 40 °C.

HeLa cells, gift of Dr. Gergely Lucaks from McGill University (Montreal, Canada) were grown in DMEM supplemented with 10% foetal bovine serum (FBS), 0.5% penicillin, 0.5% streptomycin and 0.5% of puromycin at 37°C under 5% CO₂.

2.3 Transfections and viral infections

Viral infections of MDCK cells were performed as previously described by Chu, Kings et al. Briefly, HEK 293 cells were transiently transfected with 3 µg of each of the followings: p-VPack-GP, p-VPack-VSV-G and pFB neo kAE1 WT or mutant plasmids (Stratagene), using X-tremeGENE (Roche Applied Science). The supernatant containing the virus was collected after 24 h and added to sub-confluent MDCK cells with 8 µg/ml hexadimethrine bromide (polybrene; Sigma). Twenty-four hours after infection, cells were selected with 1 mg/ml of geneticin. Knock-down of endogenous ESCRT proteins was carried out by incubating HeLa cells with the following concentration / time of doxycycline: shHRS (Hepatocyte growth factor-regulated tyrosin kinase substrate), 300 ng/ml for five days; shSTAM (Signal Transducing Adaptor Molecule), 300 ng/ml for three days; shTsg101 (Tumor susceptibility gene 101), 50 ng/ml for three days; shNT (non-targeted), 50 ng/ml for 3 days. Twenty-four hours prior to performing the experiment, HeLa cells were transiently transfected with cDNA encoding either kAE1 WT, G701D or C479W mutant cloned into the pCDNA3 plasmid using X-tremeGENE transfection reagent (by following the manufacturer's instructions) and 16 h prior to lysis, cells were incubated with 1% DMSO directly added to the culture medium, in order to rescue trafficking and function of the mutant.

2.4 Lysate preparation and western blots

MDCK or HeLa cells expressing kAE1 WT or mutant were lysed with PBS (140 mM NaCl, 2.7 mM KCl, 10 mM Na₂HPO₄, and 1.8 mM KH₂PO₄ pH 7.4) containing 1 % Triton X-100 or RIPA buffer containing PBS and 0.5% of sodium deoxycholate and 0.1% of SDS and 1/1000 protease inhibitors [leupeptin, aprotinin, pepstatin, and PMSF (Sigma)]. Protein concentrations in cell lysates were quantified by BCA assay (Hinson et al. 1988) (using bovine serum albumin (BSA); Sigma). 20 µg of proteins diluted in 2X Laemmli sample buffer (Bio-Rad) were resolved on 8 % SDS-PAGE gels. Proteins were then transferred to nitrocellulose or PVDF membranes (Bio-rad). The membranes were blocked 1

hour at room temperature with 3 % milk in TBST (5 mM Tris base, 15 mM NaCl, 0.1% Tween-20), incubated in 1% skim milk in TBST, containing mouse anti-HA primary antibody (1/1500; Covance) over night at 4°C, followed by anti-mouse secondary antibody coupled to horseradish peroxidase (HRP) for 1 hour at 20°C. Probed proteins were detected with enhanced BM chemiluminescence Blotting Substrate (POD; Roche) or ECL Prime Western Blotting Detection System (Amersham, GE) on film (Kodak) or using Carestream software. Intensities of the bands were compared using ImageJ software or Carestream software. To assess ubiquitylation of kAE1 or the interaction with Ndfip1, the anti-ubiquitin FK2 antibody (Millipore) or the anti-Flag antibody (Sigma) were respectively used for immunoblotting after immunoprecipitation with anti-HA antibody, following the same protocol described before.

2.5 Immunoprecipitation

MDCK or HeLa cells expressing kAE1 WT or mutants were lysed with PBS (140 mM NaCl, 2.7 mM KCl, 10 mM Na₂HPO₄, and 1.8 mM KH₂PO₄ pH 7.4), containing 1 % Triton X-100 and protease inhibitors [leupeptin, aprotinin, pepstatin, and PMSF (Sigma)].

Lysates were incubated with rabbit anti-HA antibody (Santa Cruz Biotechnologies) for 2 hours at 4°C followed by Protein G-sepharose. Bound proteins were eluted with Laemmli sample buffer before detection by western blot.

2.6 Immunocytochemistry

Sub-confluent MDCK cells expressing WT or mutant kAE1 were grown on glass coverslips, fixed with 4 % paraformaldehyde (Canemco Supplies) in PBS followed by incubation with 100 mM glycine in PBS (pH 8.5) to quench non-specific fluorescence. After blocking with 1 % BSA in PBS, the kAE1 proteins located at the cell surface were detected with a mouse anti-HA primary antibody (Covance) followed by an anti-mouse antibody coupled to Cy3 (Jackson

Immunoresearch Laboratories). Each antibody was used in a 1/500 dilution for 30 minutes at 20°C. Cells were then permeabilized with 0.2 % Triton X-100 in PBS for 10 minutes, blocked with 1 % BSA and incubated with mouse anti-HA primary antibody again followed by a secondary Alexa 488 antibody (Invitrogen Molecular Probes) to detect intracellular kAE1. Nuclei were stained with DAPI. Glass coverslips were then mounted on slides using 7 µl of Fluorescence Mounting Medium (DAKO).

2.7 Imaging

High resolution images were acquired using the Angstrom Illumination system (Quorum Technologies Inc.) equipped with OptiGrid structured illumination (Qioptiq), excitation and emission filter wheels (Ludl Electronic Products) and a Flash 4.0 camera (Hamamatsu). The Angstrom and associated hardware are mounted to the 100% sideport on a DMI6000 (Leica Microsystems), fully motorized inverted microscope. All hardware was controlled with Metamorph software (Molecular Devices). Alternatively, samples were examined using an Olympus IX81 microscope equipped with a Nipkow spinning-disk optimized by Quorum Technologies (Guelph, ON, Canada) and a 100 X objective.

2.8 Functional Assays

MDCK cells expressing WT or mutant kAE1 were grown on 11 x 7.5 mm glass coverslips in 6 cm diameter dishes, until 70 % confluent. Prior to the assay, cells were treated with 1 % DMSO overnight at 37°C and 2 mM leupeptin at 37°C for the last 2 hours of DMSO incubation. After washing the coverslips with serum free OptiMEM medium (Gibco), they were incubated with 10 µM BCECF-AM (Sigma) for 10 minutes at 37°C. Coverslips were then placed in fluorescence cuvettes and the cells were perfused at room temperature with: Ringer's buffer (5 mM glucose, 5 mM potassium gluconate, 1 mM calcium gluconate, 1 mM magnesium sulphate, 10 mM HEPES, 2.5 mM Na₂HPO₄, 25 mM NaHCO₃ pH 7.4) containing 140 mM chloride, followed by a chloride free medium containing 140

mM gluconate to induce intracellular alkalization. BCECF intracellular fluorescence was calibrated with K^+ -containing buffers at pH 6.5, 7.0, or 7.5, containing 100 μ M nigericin sodium salt. The Ringer's buffers were continuously perfused with air: CO_2 (19 : 1). We used a Photon Technologies International (PTI) (London, Ontario, Canada) fluorimeter to read the fluorescence changes produced from the samples. Excitation wavelengths 440 and 490 nm and emission wavelength 510 nm were used (calibrated to the fluorimeter). Rate of pH change was determined by linear regression of the initial H^+ flux (first 30 seconds), normalized to pH calibration measurements. All measurements were done using Felix software.

2.9 Statistical Analysis

All the experiments were independently repeated a minimum of three times. Experimental results are summarized as mean \pm SEM. All statistical comparisons were made using unpaired Student's t test. A P value less than 0.05 was considered statistically significant.

Chapter 3. Results

Data represented in Figure 3.2 have been collected by Jenny C. King

Data represented in Figure 3.4 have been collected by Carmen Chu

3.1 Half-life of Golgi- and ER-retained kAE1 dRTA mutants is shorter than WT

Previously we showed that 16 h of 1% DMSO treatment can partially rescue to the cell surface the Golgi-retained, dRTA-causing kAE1 G701D mutant expressed in MDCK cells (Chu, King et al. 2013), but we have not been able to completely rescue the function of this mutant. Based on these results, we hypothesized that this mutant might be rapidly internalized and degraded. To test our hypothesis we first investigated the half-life of kAE1 dRTA G701D mutant expressed in renal epithelial cells. We employed a kAE1 cDNA construct carrying a haemagglutinin epitope inserted in the third extracellular loop. As previously shown in a paper published by our group, the HA epitope has no effect on normal folding, trafficking or function of kAE1 (Chu, King et al, 2013). We showed as well that expression levels of kAE1 in infected MDCK cells decrease over a three to four week period (on average, 5 passages) (Chu, King et al, 2013).

MDCK cells stably expressing the Golgi-retained mutant kAE1 G701D, kAE1 WT as a positive control or the ER-retained mutant C479W as negative control, were incubated with 10 µg/mL of the protein synthesis inhibitor, cycloheximide (CHX), for different times up to 24 h before lysis.

After incubation, the remaining amount of kAE1 in cell lysates was quantified by immunoblot. In cell lysates from MDCK cells, kAE1 migrates as two main bands (Figure 3.1). The bottom band corresponds to protein carrying high mannose oligosaccharides (open circles) and the top band to kAE1 protein with complex oligosaccharides (closed circles) (Chu, King et al. 2013). By correlating the intensity of the bands to the intensity of the initial band (at time 0) (100% of protein) we calculated the relative protein amount at different times. Figure 3.1 indicates that in contrast with the 22 hours half-life of kAE1 wild-type (WT), the Golgi-retained G701D and the ER-retained C479W mutants have half-lives of 2 and 5 hours, respectively. These results suggest that the cellular quality-control machinery quickly detects and degrades the two kAE1 dRTA mutants. Our data are consistent with what described by Patterson et al. (Patterson, 2010)

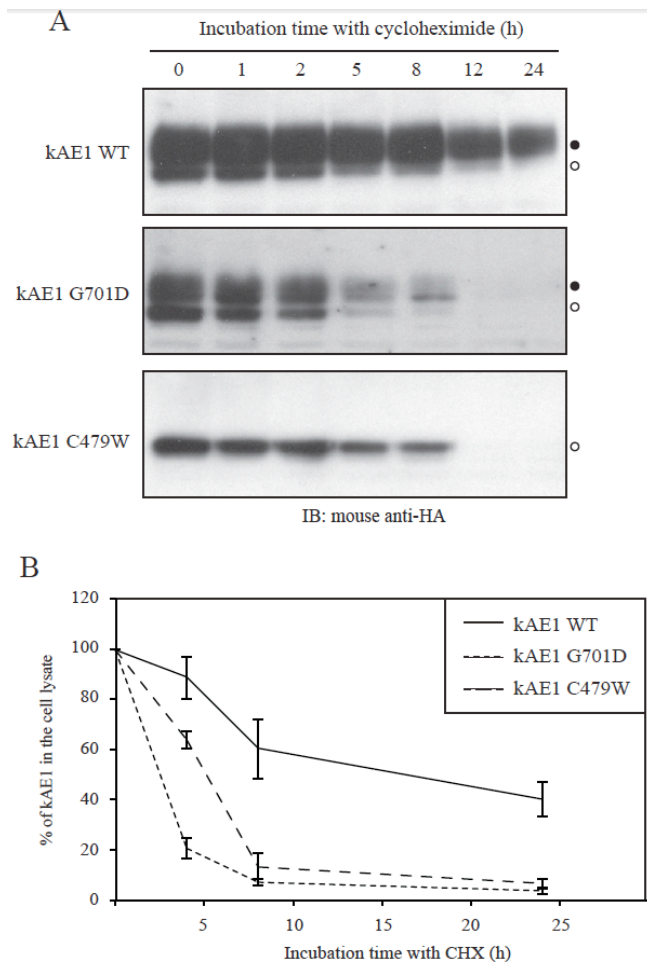


Figure 3.1. kAE1 mutants are prematurely degraded in cell lysates of MDCK cells. A, MDCK cells expressing kAE1 WT, the Golgi mutant G701D or the ER-retained mutant C479W were incubated for various lengths of time with 10 μ g/ml cycloheximide (CHX) prior to cell lysis. The same amount of protein (20 μ g) was loaded and resolved by immunoblot using a mouse anti-HA antibody. Closed circles correspond to the position of protein carrying complex oligosaccharides and open circles indicate the position of proteins carrying high mannose oligosaccharides (Chu, King et al. 2013). B, Intensities of the bands from a minimum of 3 independent experiments were compared using ImageJ software and normalized to the intrinsic control actin. Error bars correspond to SEM.

3.2 The Golgi-retained kAE1 G701D mutant is degraded by both the proteasome and lysosome

We next wondered which mechanism is involved in the degradation of the two dRTA mutants, kAE1 G701D and C479W. To investigate this, we inhibited either the proteasomal or lysosomal degradation pathway in cells expressing kAE1 WT, G701D or C479W mutants using a 2 h incubation with either 10 μ M epoxomycin or with 2 mM leupeptin, respectively. As seen on the immunoblots in Figure 3.2, analysis of lysates from cells expressing kAE1 G701D protein revealed a clear stabilization of the mutant after either of these treatments. By comparing the intensity of kAE1 bands (top and bottom), we observed a 55 ± 13 % ($n = 7$, \pm SEM) and 48 ± 15 % ($n = 6$, \pm SEM) increase of kAE1 G701D amount in the lysates after epoxomycin and leupeptin incubations, respectively. In contrast, kAE1 C479W protein expression was not significantly altered by the treatment. The stabilization of the Golgi-retained mutant by either epoxomycin or leupeptin suggests both the lysosome and proteasome participate in degradation of kAE1 G701D mutant in renal epithelial cells, and explains the premature degradation of this mutant within 2 h of protein synthesis inhibition. Interestingly, our results show no stabilization for the C479W mutant by the leupeptin treatment. This result is probably due to the fact that, as the mutant is ER-retained, it doesn't reach the further steps of biosynthesis that take place in the Golgi apparatus (see Fig. 1.5) so it is not degraded by the lysosomal pathway. We observed a slight stabilization of C479W with the epoxomycin treatment, although it was not statistically significant.

To further confirm the involvement of the lysosomal pathway in degradation of kAE1 G701D mutant, we treated MDCK cells expressing kAE1 G701D with 10 μ M or 100 μ M chloroquine, a different lysosome inhibitor (Fan et al, 2006). As shown in Figure 3.3, chloroquine has the same stabilizing effect on kAE1 G701D as leupeptin, thus confirming that the lysosome is essential in degradation of this mutant.

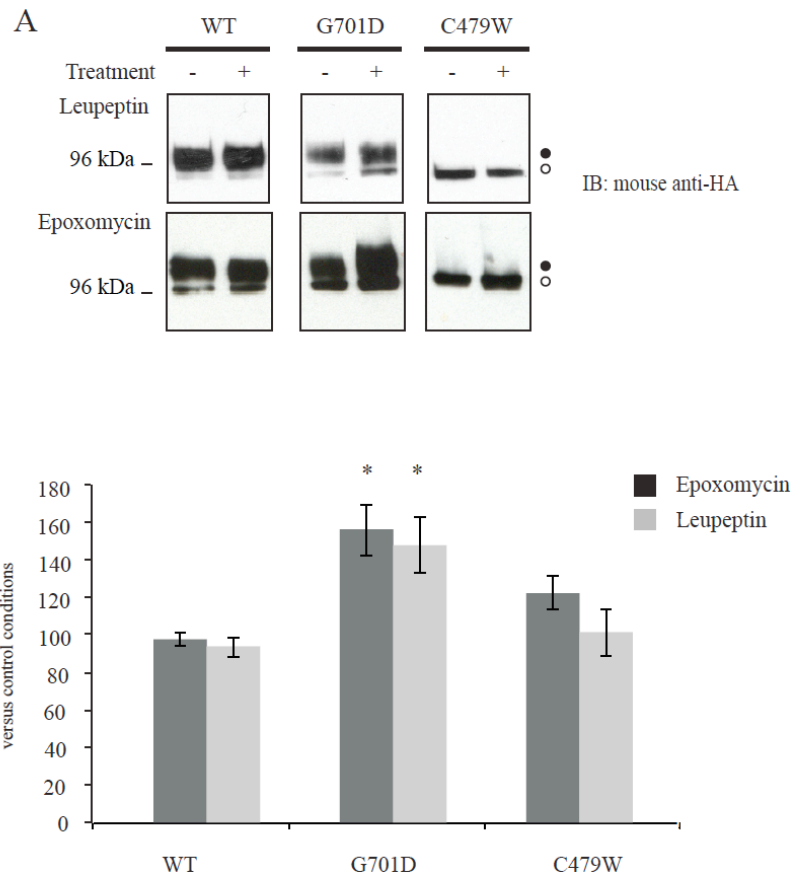


Figure 3.2. Both the lysosome and proteasome participate in the degradation of the Golgi-retained and ER retained kAE1 mutants. A, MDCK cells expressing kAE1 WT, G701D or C479W were untreated or treated with either 10 μ M epoxomycin (proteasome inhibitor) or 2 mM leupeptin (lysosome inhibitor) for 2 hours at 37°C. Proteins in the cell lysates were immunoprecipitated and resolved on SDS-PAGE gels. Eluted kAE1 proteins were detected using an anti-HA antibody by immunoblot. Closed circles correspond to the position of protein carrying complex oligosaccharides and open circles indicate the position of proteins carrying high mannose oligosaccharides. B, Percentage of kAE1 proteins present in the cell lysates after epoxomycin treatment versus control conditions, analyzed with ImageJ software. Error bars correspond to SEM, from a minimum of 3 independent experiments. * represents $p < 0.05$ versus control conditions.

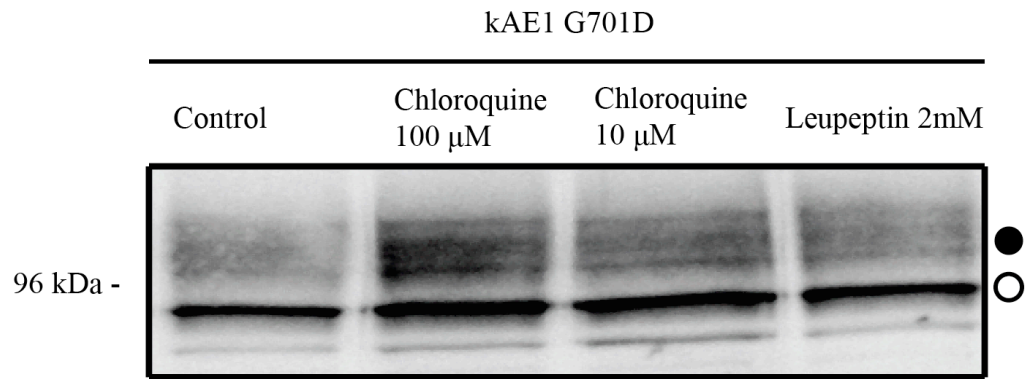


Figure 3.3. MDCK cells expressing kAE1 G701D were treated either with 10 μ M or with 100 μ M chloroquine for 2 hours at 37C. Proteins in the cell lysates were resolved on SDS-PAGE gels and detected using an anti-HA antibody by immunoblot. Closed circles correspond to the position of protein carrying complex oligosaccharides and open circles indicate the position of proteins carrying high mannose oligosaccharides.

3.3 ER-retained mutant and Golgi-retained mutant are poly-ubiquitylated upon inhibition of degradation machineries

Proteins targeted for degradation are often poly-ubiquitylated in cells (Jung and Grune 2013). MDCK cells expressing either kAE1 WT, G701D or C479W were incubated with either leupeptin or epoxomycin for 2 hours prior to lysis. We hypothesized that with such a short half-life of kAE1 mutants, a 2 h incubation of MDCK cells expressing kAE1 with the inhibitors may provide detectable changes in the stability and ubiquitylation of the protein. After cell lysis with 1 % Triton X-100 lysis buffer, kAE1 proteins were immunoprecipitated and ubiquitylated kAE1 molecules were identified by immunoblotting with an anti-ubiquitin antibody. We found that both epoxomycin and leupeptin treatment increased the amount of poly-ubiquitylated kAE1 protein (Figure 3.4), in addition to stabilizing the amount of kAE1 protein remaining in the lysates (Figure 3.2). Interestingly, the leupeptin treatment seemed to increase poly-ubiquitylation of kAE1 G701D more prominently, while epoxomycin treatment resulted in a denser smear of poly-ubiquitylated kAE1 C479W.

Figure 3.5 represents the result of the same experiment performed using radioimmunoprecipitation assay buffer (RIPA buffer), more denaturing than Triton X-100 because it contains sodium deoxycholate (Ngoka et al. 2008). The purpose was to make sure that the smear observed in figure 8A was really due to poly-ubiquitylated kAE1 and not to ubiquitylated kAE1-interacting proteins, still bound to kAE1 after lysis with Triton X-100.

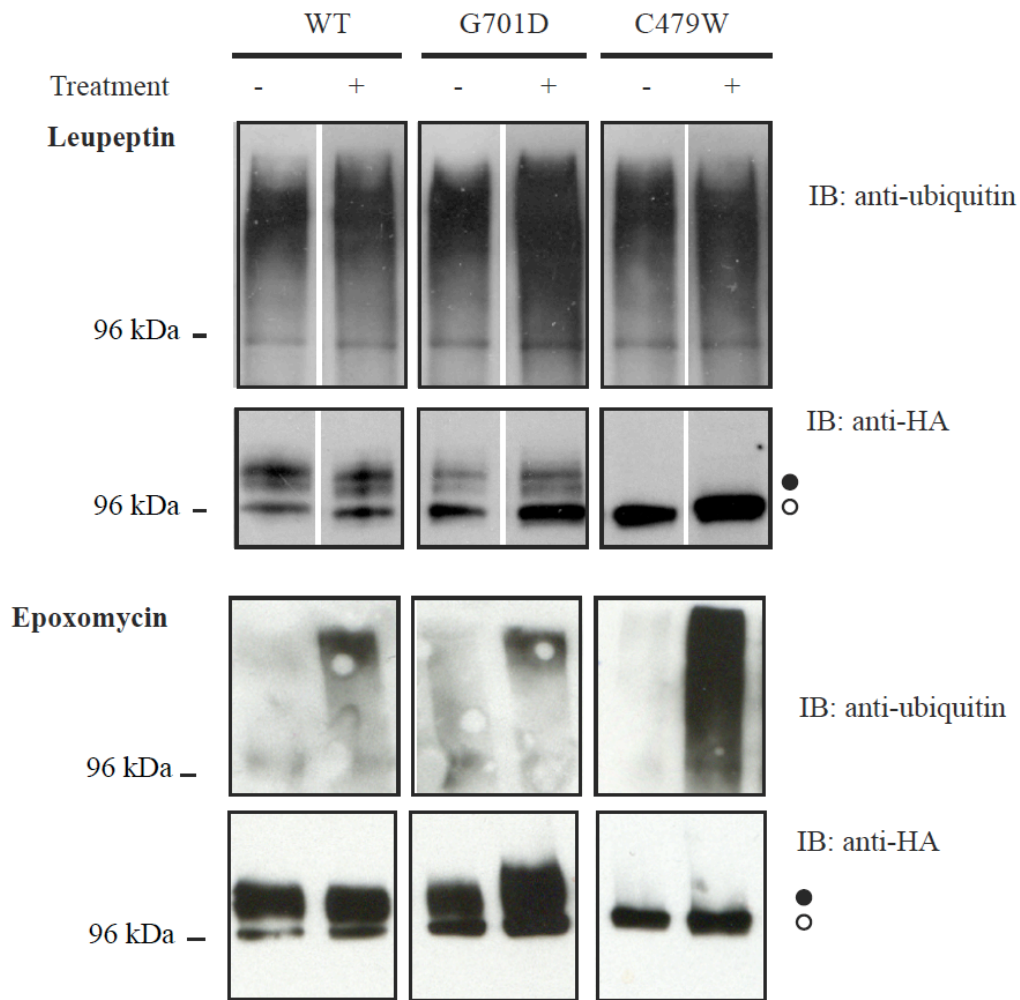


Figure 3.4. kAE1 dRTA mutants are poly-ubiquitylated. MDCK cells expressing either kAE1 WT, G701D or C479W were incubated for 2 hours at 37°C with either leupeptin (top panels) or epoxomycin (bottom panels). Cell lysis was performed using a buffer containing Triton X-100. Immunoprecipitated kAE1 proteins were then resolved by SDS PAGE gels and immunoblotted with anti-ubiquitin antibody. Top 6 panels correspond to Leupeptin treatment, bottom 6 panels show epoxomycin treatment. Closed circles correspond to the position of protein carrying complex oligosaccharides and open circles indicate the position of proteins carrying high mannose oligosaccharides.

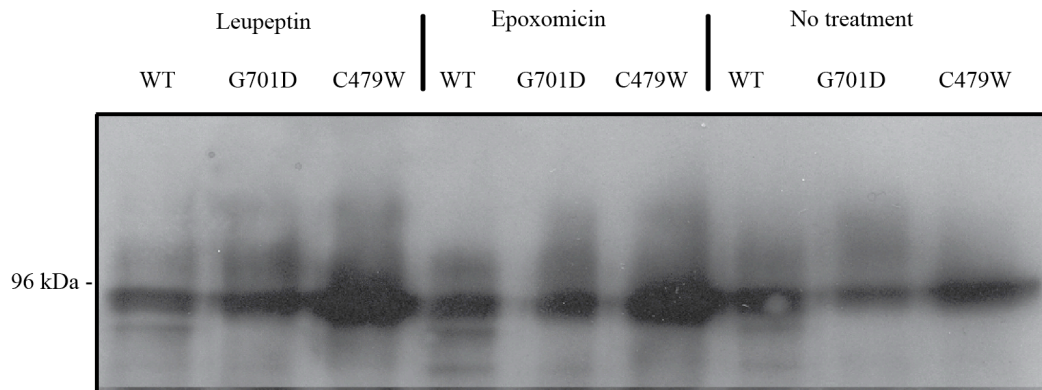


Figure 3.5. kAE1 dRTA mutants are poly-ubiquitylated. MDCK cells expressing either kAE1 WT, G701D or C479W were incubated for 2 hours at 37°C with either leupeptin or epoxomicin. Cell lysis was performed using a buffer containing deoxycholate and SDS (RIPA buffer). Immunoprecipitated kAE1 proteins were then resolved by SDS PAGE gels and immunoblotted with anti-ubiquitin antibody.

These experiments indicate that a functional ubiquitin machinery is necessary for degradation of kAE1 WT or dRTA mutants and support that dRTA mutants are more heavily poly-ubiquitylated than kAE1 WT, consistent with their premature degradation. As little is known about the degradation machinery of membrane proteins in the Golgi, we next investigated the degradation mechanisms of the Golgi-retained kAE1 G701D mutant.

3.4 The Golgi-retained kAE1 G701D mutant transiently reaches the plasma membrane prior to degradation

After having demonstrated that both lysosomes and proteasomes are involved in kAE1 G701D mutant degradation, we investigated the mechanisms by which the mutant could be prematurely degraded. We formulated three hypotheses:

- 1) The Golgi-retained kAE1 G701D mutant is loaded into intracellular vesicles trafficking from the Golgi directly to lysosomes.
- 2) The mutant is targeted to the lysosomes after having reached the plasma membrane.
- 3) The mutant is moved back to the ER for proteasomal degradation.

To discriminate between hypotheses 1 and 2, we determined whether kAE1 G701D dRTA mutant ever reaches the plasma membrane of intact, live MDCK cells, by taking advantage of the extracellular HA epitope in the third extracellular loop of kAE1. We incubated live, untransfected MDCK cells or MDCK cells expressing kAE1 WT, G701D or C479W either with an anti-actin antibody as a control or with an anti-HA antibody for 1 hour at 37°C. The anti-HA antibody detects the HA epitope located in the third extracellular loop of kAE1 if it is targeted to the plasma membrane. After a one hour incubation, cells were fixed, permeabilized and primary antibodies were detected using a secondary Cy3 (red)-coupled antibody. Figure 8 shows specific staining of both cell surface and intracellular vesicles for kAE1 WT (Figure 3.6, panel A), and staining of intracellular vesicles for kAE1 G701D (panel C). In contrast, neither

intact MDCK cells incubated with mouse anti-HA antibody nor MDCK cells expressing kAE1 G701D incubated with anti-actin antibody displayed similar intracellular or plasma membrane staining (Figure 3.6, panels D & E).

These results indicate that, although predominantly retained in the Golgi at the steady-state, the kAE1 G701D mutant transiently reaches the plasma membrane but is endocytosed in intracellular vesicles within one hour. By comparing the intensity of kAE1 staining (red) located at the plasma membrane in WT (panel A, arrowheads) versus the absence of cell surface staining for kAE1 G701D (panel C), we hypothesize that kAE1 G701D is prematurely endocytosed compared with kAE1 WT.

We next investigated whether kAE1 G701D mutant under trafficking rescuing conditions with 1 % DMSO incubation, was also endocytosed within one hour. We incubated either control MDCK cells or MDCK cells expressing kAE1 G701D with 1 % DMSO for 16 hours to rescue trafficking of the mutant to the cell surface and then followed the same protocol as described above. Upon partial rescue of cell surface trafficking of the mutant, we observed that kAE1 G701D was still predominantly endocytosed within one hour (Figure 3.6, panel B). These results indicate that although predominantly retained in the Golgi, the G701D kAE1 mutant transiently reaches the plasma membrane from where it is quickly endocytosed and accumulated in intracellular vesicles within 1 hour.

3.5 The endocytosed kAE1 G701D mutant colocalizes with lysosomes

We hypothesized that the kAE1 G701D mutant, after having reached the plasma membrane and been endocytosed, is then degraded by the lysosomal pathway.

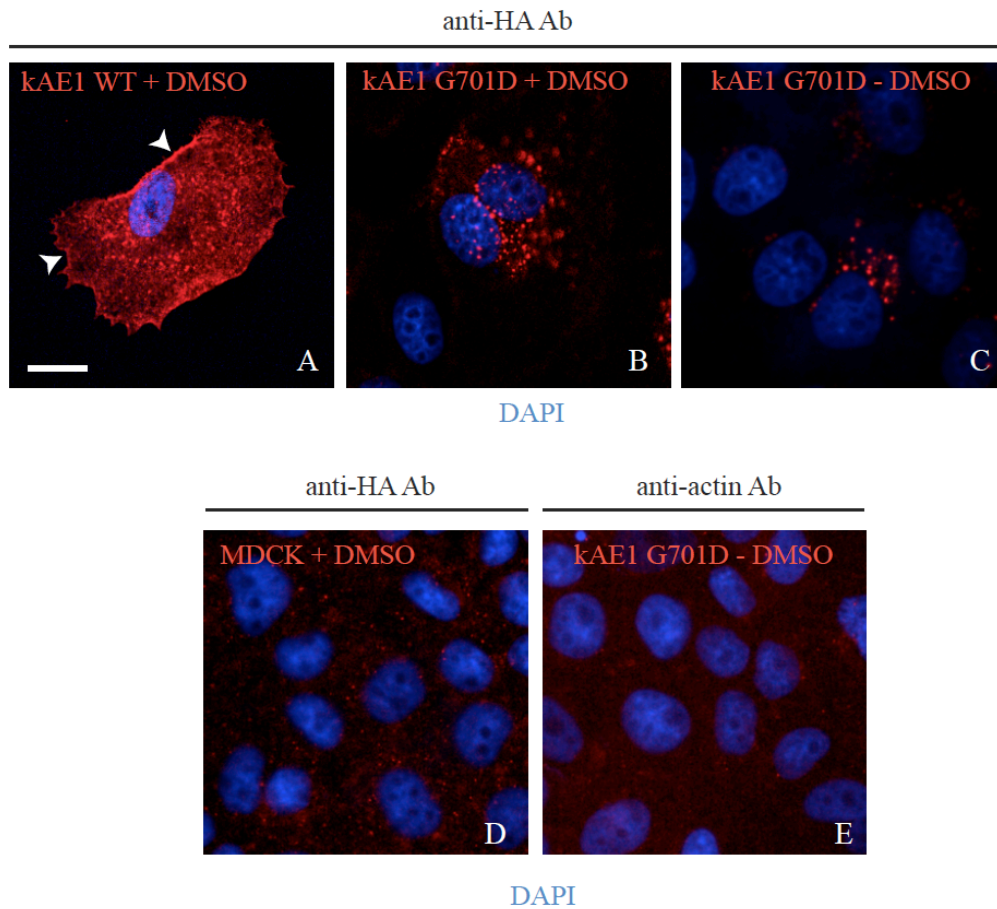


Figure 3.6. kAE1 G701D mutant transiently reaches the plasma membrane. MDCK cells expressing either kAE1 WT or G701D were incubated for 16 hours with 1 % DMSO at 37°C. Cells were then incubated with mouse anti-HA or mouse anti-actin antibodies for 1 h at 37°C, prior to fixation, permeabilization and staining with an anti-mouse antibody coupled to Cy3. The nuclei were stained with DAPI. The slides were imaged with an Olympus microscope coupled to a DG4 lamp and using a 40 X objective. Bar corresponds to 10 μ m.

To investigate the fate of endocytosed kAE1 G701D mutant, we transiently transfected MDCK cells expressing kAE1 WT or G701D with lysosomal-associated membrane protein-1 (Lamp-1) cDNA fused to the venus fluorescent protein. MDCK cells expressing either kAE1 WT or G701D and transiently transfected with Lamp-1 were incubated with mouse anti-HA antibody for 2 hours at 37°C, prior to fixation, permeabilization and detection of primary antibody with anti-mouse antibody coupled to Cy3 fluorophore. Examination of the cells revealed that endocytosed kAE1 G701D partially co-localized with the lysosomal marker Lamp-1 in a peri-nuclear location (Figure 3.7, bottom right of top panel, arrowheads). In contrast, there was minimal overlap of the staining between endocytosed kAE1 WT and Lamp-1 proteins (Figure 3.7, top panels), and instead, a high level of co-localization with the recycling endosome marker transferrin after a three hours incubation of intact, living cells with the mouse anti-HA antibody (Figure 3.7, top right of bottom panels). Endocytosed kAE1 G701D did not show an obvious colocalization with transferrin (Figure 3.7, bottom right of bottom panels). Although it is possible that over-expression of the lysosomal marker or the presence of venus fluorescent protein alters the final location of the lysosomal protein, these results support the conclusion that after endocytosis, the kAE1 G701D mutant is targeted to the lysosome for degradation.

3.6 Knocking down components of the peripheral quality-control machinery stabilizes rescued kAE1 G701D mutant

As previously discussed, endocytosed proteins are sorted to late endosomes and lysosomes where they are degraded (van Meel and Klumperman 2008). The sorting of endocytosed membrane proteins involves a peripheral quality-control machinery composed of four types of endosomal sorting complex for transport (ESCRT) (Okuyoneda, Barriere et al. 2010). Vaccari et al. have recently investigated the role of individual components of the peripheral quality-control ESCRT machinery (Vaccari, Rusten et al. 2009). ESCRT machinery comprises a

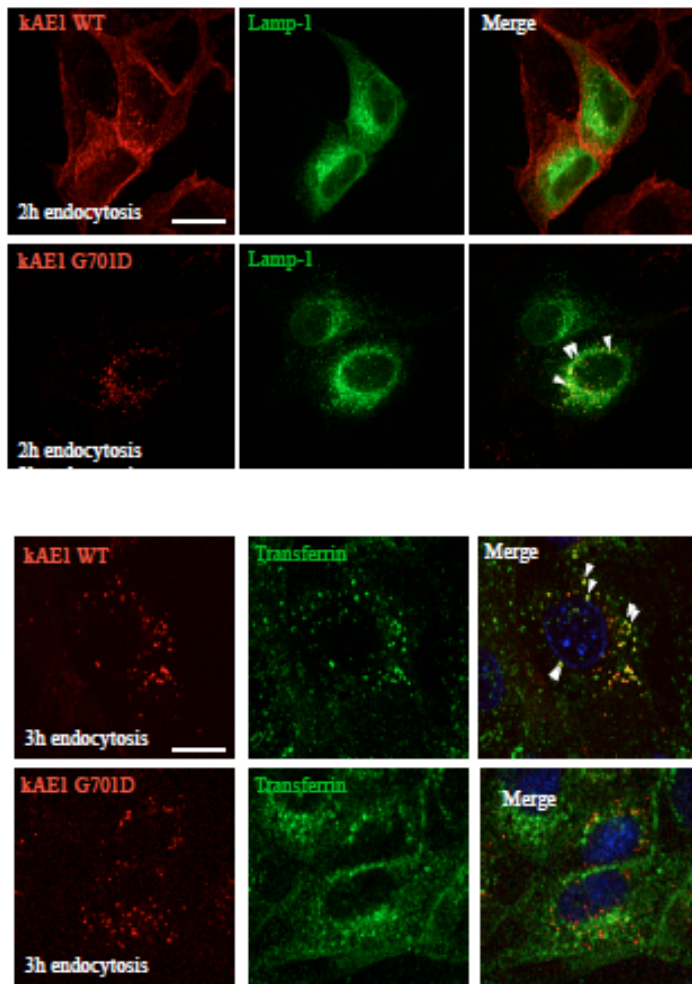


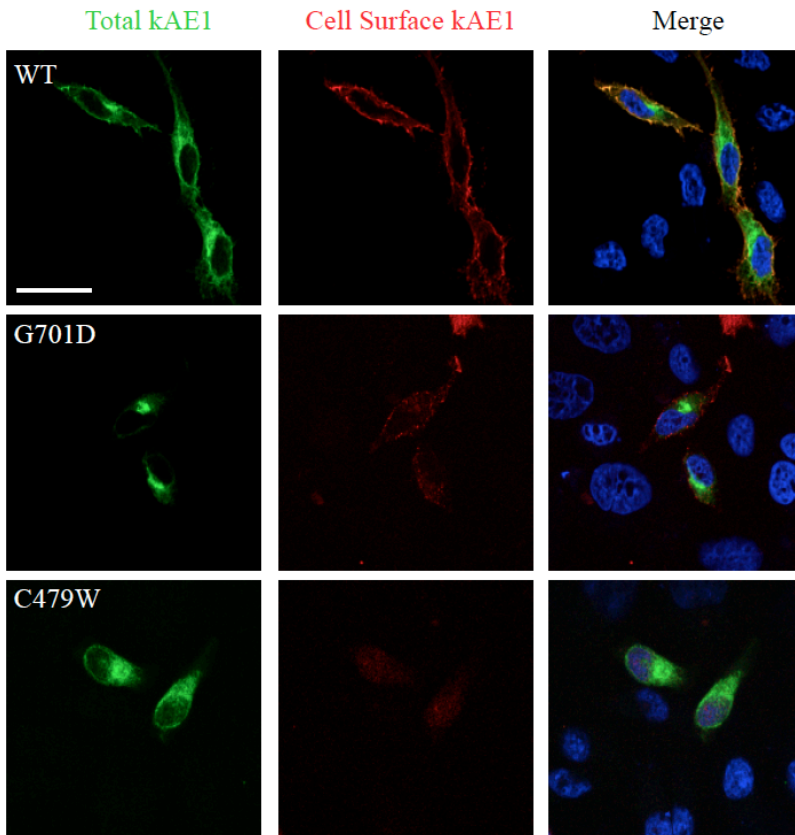
Fig 3.7. Endocytosed kAE1 G701D mutant partially co-localizes with lysosomal marker Lamp-1. MDCK cells expressing kAE1 WT or G701D, transiently transfected with cDNA encoding the lysosomal marker Lamp-1 fused to Venus fluorescent protein, were incubated with mouse anti-HA antibody for 2 hours at 37 °C (top panels). After fixation, kAE1 proteins were detected with an anti-mouse antibody coupled to Cy3 fluorophore. For colocalization with transferrin receptor (bottom panels), MDCK cells expressing kAE1 WT were starved for 1 hour before addition of transferrin coupled to Alexa 488 and mouse anti-HA antibody to the medium for 3 hours at 37°C. Cells were fixed, permeabilized and primary antibody was detected with anti-mouse antibody coupled to Cy3 fluorophore. Samples were examined by fluorescence microscopy using a 63 X objective. Nuclei were stained with DAPI. Bar corresponds to 10 μ m.

number of essential components for peripheral quality-control, including Hepatocyte growth factor-regulated tyrosine kinase substrate (Hrs), Signal-Transducing Adaptor Molecule (STAM), and Tumor susceptibility gene 101 (Tsg101). As both rescued and non-rescued Golgi-retained kAE1 G701D transiently reach the plasma membrane (Figure 3.6), we next asked whether these components of the peripheral quality-control machinery are involved in premature degradation of kAE1 G701D.

We transiently transfected HeLa cells that are knocked down for either Hrs, STAM, TSG101 or that express non-targeting shRNA (HeLa NT) with kAE1 WT, G701D or C479W, incubated with 1 % DMSO for 16 hours.

We first performed an immunofluorescence experiment to confirm that kAE1 reached the surface in these cells. We detected cell surface kAE1, using the extracellular HA epitope prior to cell permeabilization (Figure 3.8 A, red). After cell permeabilization, total kAE1 is shown in green. As shown by the red staining on Figure 3.8 A, kAE1 WT reaches the plasma membrane in HeLa cells. Less kAE1 G701D protein reaches the cell surface as shown by the less intense red staining compared with kAE1 WT. After permeabilization, staining of total kAE1 G701D shows a perinuclear localization, reminiscent of the Golgi localization of this mutant in MDCK and LLC-PK1 cells (Chu, King et al. 2013). No surface (red) staining was seen on cells transfected with the ER-retained kAE1 C479W mutant, indicating that overall, the kAE1 WT or mutants trafficked in a similar way in HeLa or MDCK cells. We then analyzed the relative amount of kAE1 WT or mutant proteins 24 hours post-transfection by immunoblot in the various HeLa cell lines. Immunoblot and quantification results on Figure 3.8 B & C indicate that both the amount of kAE1 WT and G701D were increased when these essential components were down-regulated. In contrast, the amount of ER-retained kAE1 C479W remained mostly unchanged, except when expressed in cells knocked-down for Hrs. Note that in these HeLa cells, kAE1 is resolved as a single band in contrast with the two bands seen in MDCK cells, suggesting that in these cells, kAE1 glycosylation is different from MDCK cells.

A



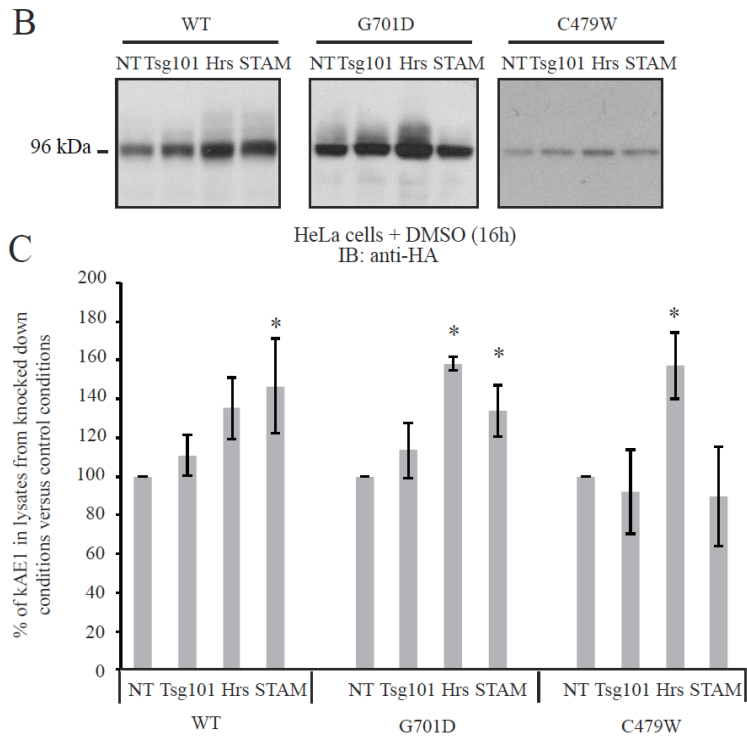


Fig 3.8. Knocking-down components of the peripheral quality-control machinery stabilizes kAE1 G701D. Control HeLa cells (NT) or knocked down for Hrs, STAM or Tsg101 proteins were transiently transfected with kAE1 WT, G701D or C479W. Sixteen hours prior to lysis, cells were incubated with 1 % DMSO.

A, the localization of kAE1 WT, G701D and C479W was determined by immunofluorescence, by detecting cell surface kAE1 before permeabilization in red and total kAE1 after permeabilization in green. The samples were examined using a Leica microscope coupled to an Angstrom illumination system with a 40X oil objective. Bar corresponds to 10 μ m.

B, The steady-state amount of kAE1 was investigated by immunoblot using a mouse anti-HA antibody. C, Intensities of kAE1 bands from the various cell lines were compared using ImageJ software and the percentage of kAE1 present in treated versus control conditions are shown in the histogram. NT corresponds to HeLa cells treated with non-targeting shRNAs. Note that in these HeLa cells, kAE1 is resolved as a single band in contrast with the two bands seen in MDCK cells, suggesting that in these cells, kAE1 glycosylation is different from MDCK cells. Error bars correspond to SEM, from a minimum of 3 independent experiments. * represents $p < 0.05$ versus NT conditions.

These results support that premature degradation of kAE1 G701D occurs via a peripheral quality control machinery-dependent mechanism.

3.7 Inhibiting the lysosome restores the function of kAE1 G701D mutant

As incubating cells expressing kAE1 G701D with a lysosomal inhibitor markedly increased the total amount of the mutant in MDCK cells (Figure 3.2), we next examined whether inhibition of the lysosome would rescue the function of kAE1 G701D at the surface of MDCK cells. To obtain the maximal functional rescue, the cells were first incubated for 16 hours with 1 % DMSO to enhance kAE1 G701D surface trafficking, then complemented this medium with 2 mM leupeptin for the last 2 hours of incubation to inhibit the lysosome. We performed a fluorescence-based functional assay by monitoring intracellular pH variations in control MDCK cells or cells expressing kAE1 WT or G701D, using the ratiometric fluorescence-based pH sensitive dye 2',7'-Bis(2-carboxyethyl)-5(6)-carboxyfluorescein-acetoxymethyl ester (BCECF-AM). Cells expressing either proteins were first incubated for two hours with 2 mM leupeptin at 37°C (Chu, King et al. 2013). After pre-loading the cells with BCECF-AM in the presence of chloride, we perfused them with a chloride-free Ringer's buffer in the presence of extracellular bicarbonate. If kAE1 is functional and present at the cell surface, entry of bicarbonate through kAE1 results in an increase of intracellular pH and subsequently augments the intracellular BCECF fluorescence. The bicarbonate-chloride transport rate in the initial 30 seconds of activity was measured and compared to non-treated conditions. Then, we perfused the cells with three nigericin-containing buffers at three different pH levels (6.5, 7.0, 7.5) in order to correlate a fluorescence intensity to a pH value. As seen on Figure 3.9, treatment with DMSO and leupeptin significantly increased the functional activity of kAE1 G701D from $0.060 \pm 0.017 \Delta \text{pH}/\text{min}$ ($n = 4, \pm \text{SEM}$) to $0.107 \pm 0.010 \text{ mM}/\text{min}$

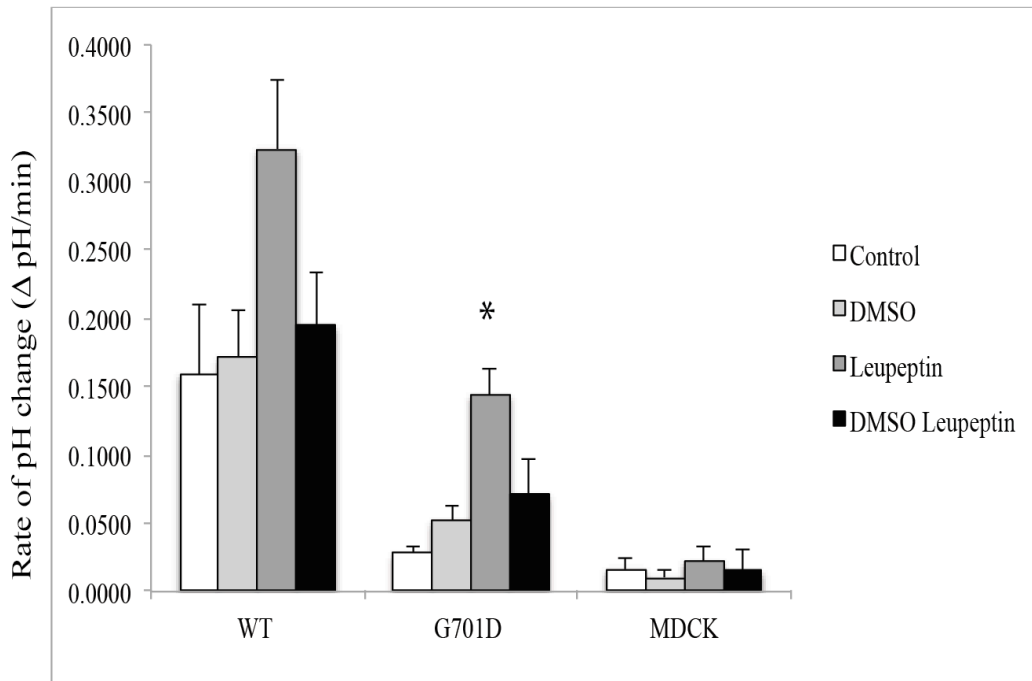


Fig 3.9. MDCK cells expressing kAE1 WT and G701D were incubated for 16 hours at 37°C with 1 % DMSO and with 2 mM leupeptin for the last 2 hours of DMSO incubation. After loading cells with BCECF, coverslips placed in a fluorescence cuvette were perfused with a Ringer's solution containing sodium chloride at room temperature. Upon switching to a chloride-free solution, the fluorescence increase was recorded and the rate of increase over the first 90 seconds was measured. BCECF fluorescence was calibrated to intracellular pH using high-potassium buffers containing nigericin at three different pH. Values correspond to means, error bars to SEM, from a minimum of three independent experiments. (*) marks a significant difference between the leupeptin treatment and the DMSO treatment for kAE1 G701D mutant. An immunofluorescence assay was performed for each single experiment to verify the expression of kAE1.

(n = 5, ± SEM). There was no longer a significant difference of transport rate between kAE1 WT and kAE1 G701D mutant after incubation of the cells with DMSO and leupeptin.

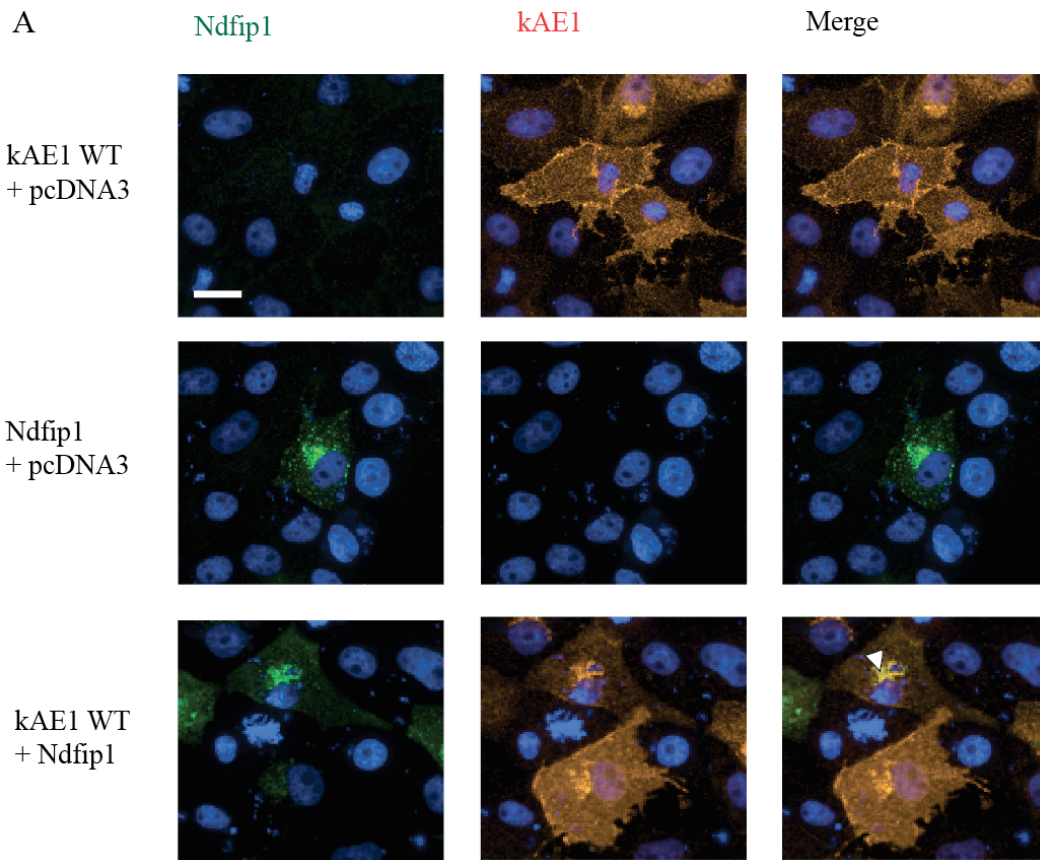
These results support the conclusion that inhibiting lysosomal degradation promotes an increased functional activity of the kAE1 G701D mutant in renal epithelial cells. Interestingly, the absence of DMSO did not produce any decrease in kAE1 G701D mutant functional activity, thus suggesting that the leupeptin treatment is sufficient by itself to promote the increase of activity.

3.8 Ndfip1 interacts with kAE1 G701D mutant

As previously discussed, ubiquitin ligases of the Nedd4 family are important for ubiquitylation processes downregulating the expression of cell surface proteins such as the epithelial sodium channel (ENaC) in the collecting duct of the kidneys (Kumar, Harvey et al. 1997). Nedd4 family-interacting protein1 (Ndfip1) is an ubiquitin ligase adaptor, which, in yeast, is located in the Golgi, where it detects polar residues within transmembrane domains (Goh, Low et al. 2013). The exact position of the 701 residue is still controversial: Bonar et al. have developed a 13 transmembrane domains-model of AE1 where the 701 residue is located on the ninth cytosolic loop (Bonar and Casey, 2008).

Nevertheless, based on our model, kAE1 G701D introduces a charged aspartate in the ninth transmembrane domain. For this reason we hypothesized that kAE1 G701D interacts with Ndfip1 and that Ndfip plays a role in the premature degradation of this dRTA mutants.

To investigate this possibility, we first asked whether the two proteins colocalize in mammalian cells. We performed an immunofluorescence assay on LLC-PK1 cells co-transfected with kAE1 HA-tagged and Ndfip1 Flag-tagged. We used LLC-PK1 cells instead of MDCK due to higher transfection efficiency with Ndfip1. Cells were fixed, permeabilized and incubated with a mouse anti-Flag antibody and a rat anti-HA antibody. Anti-mouse Alexa 488 and anti-rat Cy3



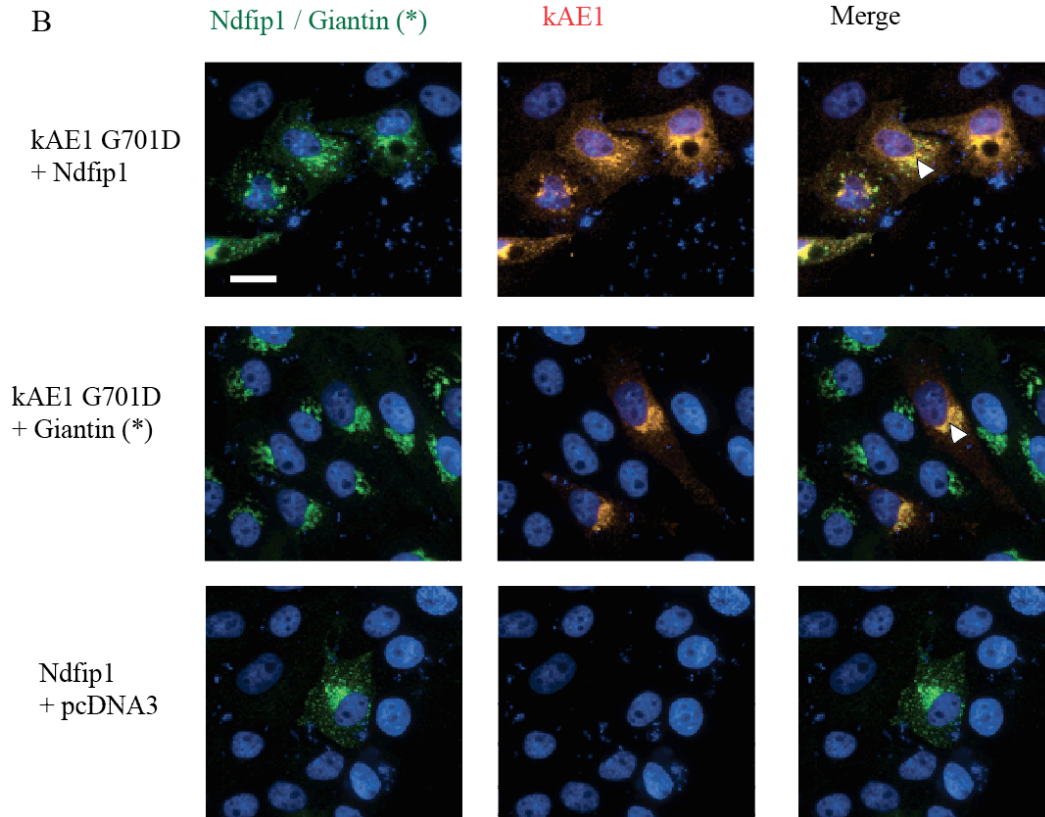


Fig. 3.10. LLC-PK1 cells were co-transfected with kAE1 WT (A) or kAE1 G701D (B) HA-tagged and Ndfip1 Flag-tagged. Cells were then permeabilized and incubated with rat anti-HA / anti-rat Cy3 and with mouse anti-Flag or anti-Giantin / anti-mouse AlexaFluor 488. The nuclei were stained with DAPI. The slides were imaged with an Olympus microscope coupled to a DG4 lamp and using a 60 X objective. Arrowheads on the right panels point to yellow staining, corresponding to colocalization of kAE1 G701D and Ndfip1. Bar corresponds to 10 μ m.

antibodies were used as secondary antibodies (Figures 3.10 and 3.11). The immunofluorescence assay confirmed that kAE1 G701D mutant is mainly intracellular while WT protein is expressed at the cell surface. Moreover, we were able to detect a colocalization between kAE1 G701D and the Golgi marker Giantin, thus confirming that kAE1 G701D is mainly Golgi-retained (Figure 3.11) (Chu, King et al. 2013). Furthermore, the immunofluorescence showed a colocalization between kAE1 G701D and Ndfip1, consistent with the hypothesis that Ndfip1 resides in the same compartment than kAE1 G701D and may be involved in the ubiquitylation process of kAE1.

In order to further confirm our findings, we co-transfected LLC-PK1 cells with kAE1 WT or G701D mutant together with Ndfip1-Flag tagged. After lysis, kAE1 proteins were immunoprecipitated using a rabbit anti-HA antibody and detected by immunoblotting with a mouse anti-HA antibody. Ndfip1 proteins eventually bound to kAE1 were then identified by immunoblotting with an anti-Flag antibody. Figure 3.11 shows 27 kDa bands which corresponds to the expected molecular weight of Ndfip1 protein, when kAE1 (WT or G701D mutant) were co-expressed with Ndfip1. In absence of Ndfip1, no 27 kDa band is observed. The positive control (last lane) shows an interaction between kAE1 WT HA-tagged and kAE1 WT Myc-tagged, as kAE1 is known to dimerize (Cordat 2006).

These results show an interaction between kAE1 and Ndfip1, suggesting that Ndfip1 is involved in the kAE1 ubiquitylation process. Figure 3.11 clearly shows a more intense band where Ndfip1 was coexpressed with kAE1 G701D compared to where Ndfip1 was coexpressed with kAE1 WT, suggesting a stronger interaction of Ndfip1 with kAE1 G701D mutant. Quantification of kAE1 interacting Ndfip1 band intensities showed indeed that the Ndfip1 band is twice as intense when coexpressed with kAE1 G701D compared to when coexpressed with kAE1 WT. This observation is consistent with a faster degradation of the mutant.

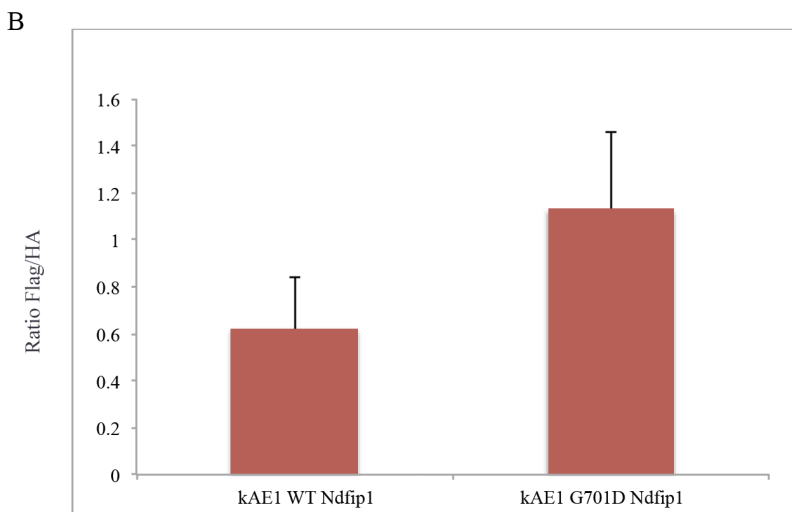
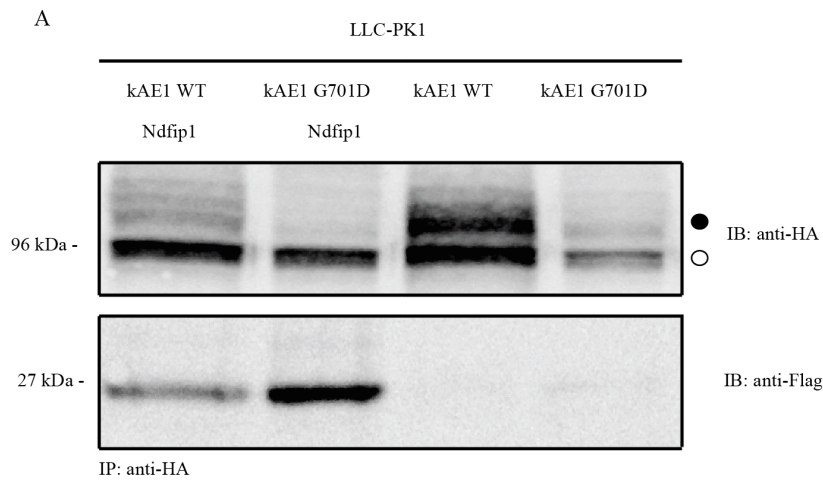


Fig. 3.11. LLC-PK1 cells co-expressing kAE1 and Ndfip1 were lysed. A kAE1 proteins present in cell lysates were immunoprecipitated using an anti-HA antibody. The presence of kAE1 was detected by immunoblotting with anti-HA antibody (upper panel), while Ndfip1 eventually bound to kAE1 and thus immunoprecipitated with it was detected by immunoblotting with an anti-Flag antibody (lower panel). Closed circles correspond to the position of protein carrying complex oligosaccharides and open circles indicate the position of proteins carrying high mannose oligosaccharides.

B The graph represent the ratio between the fluorescence intensity of the 27 kDa band and the one of the 96 kDa band.

Chapter 4. Discussion

The interest about kAE1 G701D mutant rises from the fact that proteins with this mutation are functional in erythrocytes where it is likely properly targeted to the cell surface by the chaperone activity of glycophorin A (Wu, Satchwell et al. 2011). In type A intercalated cells, the lack of glycophorin A leads to a mistargeting of this mutant which remains in the Golgi apparatus and this results in distal renal tubular acidosis. This is the situation seen in homozygous patients carrying kAE1 G701D mutant, whose type-A intercalated cells contain kAE1 G701D homodimer proteins. However, in heterozygous patients, since kAE1 WT exhibits a dominant-positive effect on the recessive mutants (Bruce et al, 2000), kAE1 G701D can heterodimerize with the WT protein and thus be able to properly traffic to the plasma membrane (Yenchitosmanus et al. 2005). Moreover, a Golgi-based quality control mechanism has been described in yeast (Bagnat et al. 2001), but the degradation mechanisms of non-native Golgi-retained mutated proteins are not characterized in mammalian cells. Therefore, the kAE1 G701D mutant represents a unique opportunity to learn more about Golgi-located degradation mechanisms in mammalian cells.

4.1 kAE1 G701D and C479W are prematurely degraded

In our work, we demonstrated that the incomplete functional activity of kAE1 G701D observed after its rescue by DMSO treatment (Chu, King et al. 2013) is due to its rapid degradation (Figure 3.1). Indeed, using epithelial cells that express kAE1 WT or mutant, and incubated with the protein synthesis inhibitor cycloheximide (Figure 3.1), we calculated a half-life of 22 hours for the WT protein in contrast with 4 hours for the kAE1 G701D mutant.

The premature degradation of kAE1 G701D occurs via both the lysosomal and the proteosomal degradation pathways, since both leupeptin-mediated lysosome inhibition and epoxomicin-mediated proteosomal inhibition stabilize kAE1 G701D (Figure 3.2). The advantage of using epoxomicin, compared to

other proteasome inhibitors, is that epoxomicin does not inhibit nonproteasomal proteases, thus being absolutely specific (Meng, Mohan et al. 1999). Furthermore, it is an irreversible inhibitor of the proteasome (Meng, Mohan et al. 1999). To confirm the effect of lysosomal inhibition by leupeptin, we demonstrated that the same kAE1 stabilization occurs in chloroquine-mediated lysosome inhibition (Figure 3.2). The lysosomes mainly degrade proteins endocytosed from the cell surface, while misfolded or mutated proteins in the ER are mainly degraded by the proteasomal pathway (Clague and Urbe 2010). We hypothesize that the proteasome contributes to degradation of the kAE1 G701D proteins that have not reached the Golgi maturation step yet. Alternatively, Golgi-located kAE1 G701D mutant may traffic back to the endoplasmic reticulum from the Golgi before being retro-translocated and degraded by the proteasome.

The ER-retained mutant kAE1 C479W is also prematurely degraded (Figure 3.1), mainly via proteosomal pathway (Figure 3.2). Interestingly, the leupeptin treatment seems to have no effect on the stabilization of kAE1 C479W. This could be explained by the fact that this mutant does not reach the maturation steps beyond the ER and for this reason inhibiting the lysosomal degradation pathway has no effect on it.

4.2 kAE1 G701D mutant is poly-ubiquitylated

The immunoprecipitation-immunoblotting assay shown in Figure 3.4 indicates that a functional ubiquitin machinery is necessary for degradation of kAE1 WT or the two dRTA mutants studied. It also showed that dRTA mutants are more heavily poly-ubiquitylated than kAE1 WT, consistently with their premature degradation.

This experiment was performed by immunoprecipitating kAE1 in MDCK cell lysates with an anti-HA antibody. We expected to observe a clear smear, representing kAE1 bound to different numbers of ubiquitin, by immunoblotting with both anti-HA and anti-ubiquitin antibodies. Interestingly, we observed a

clear smear only when we blotted with anti-ubiquitin antibody. No smear was observed when we blotted with anti-HA antibody.

These findings suggest that, even if we immunoprecipitated kAE1 with an anti-HA antibody before resolving our samples on SDS-PAGE gel, the anti-ubiquitin antibody detected some ubiquitylated proteins different than kAE1. This hypothesis is supported by the fact that kAE1 interacts with other proteins such as the integrin-linked kinase (Keskanokwong, Shandro et al. 2007), GAPDH, Carbonic Anhydrase II, Adaptor Proteins (Almomani, King et al. 2012) and probably many other un-identified ones that may be ubiquitylated when we lysed the cells. This would explain why the cluster of molecules present throughout the gel lane is recognized by the anti-ubiquitin antibody but not by the anti-HA antibody. The buffer we used for cell lysis contains 1 % Triton X-100, a detergent that does not disrupt interactions between kAE1 and different proteins. So, by immunoprecipitating with an anti-HA antibody, we have probably not just precipitated kAE1 but some kAE1-interacting proteins as well and we hypothesize this is the reason why we obtained a smear by immunoblotting with anti-ubiquitin antibody but not when we blotted with anti-HA antibody. To confirm our hypothesis, the experiment was repeated using a lysis buffer containing 0.5% of sodium deoxycholate and 0.1% of SDS (RIPA buffer), two more denaturing detergents than Triton X-100 (Ngoka et al. 2008). The experiment gave us a visible smear (Figure 3.5), even if less evident than the one obtained after lysis with Triton X-100 (Figure 3.4), thus suggesting that the smear observed in Figure 3.4 is probably due not only to polyubiquitylated kAE1, but as well to ubiquitylated kAE1 interacting proteins. A second hypothesis to explain the absence of a smear when we blotted with anti-HA antibody (Figure 3.4) is that a small percentage of total kAE1 is ubiquitylated. If this is the case, the anti-HA antibody incubation would not give us a visible smear at molecular weights higher than 96 kDa.

4.3 kAE1 G701D transiently reaches the cell surface

As discussed before, we formulated three different hypotheses to describe the degradation steps of kAE1 G701 mutant:

- 1) The Golgi-retained kAE1 G701D mutant is loaded into intracellular vesicles trafficking from the Golgi directly to lysosomes.
- 2) The mutant is targeted to the lysosomes after having reached the plasma membrane.
- 3) The mutant is moved back to the ER for proteasomal degradation.

The immunofluorescence assay shown in Figure 3.6 confirmed that kAE1 G701D mutant transiently reaches the cell surface before being internalized and degraded. Interestingly, we found that a small amount of kAE1 G701D protein can reach the cell surface even in absence of DMSO treatment (Figure 3.6 C). This finding is consistent with our finding on the immunoblotting assay shown in Figure 3.2: even without DMSO treatment, leupeptin shows its stabilizing effect, thus indicating that even in this case the lysosomal pathway is involved in kAE1 G701D degradation. The immunofluorescence shown in figure 3.6 includes as well a control with MDCK cells treated with DMSO and incubated with anti-actin antibody (not shown in the picture). The purpose of this control is to make sure that the 1 % DMSO treatment does not permeabilize the plasma membrane. Since we had no red staining in this condition, we concluded that the DMSO treatment does not affect the integrity of the plasma membrane.

Immunofluorescence assays showed that after being internalized from the cell surface, kAE1 G701D colocalizes with the lysosome-marker Lamp-1 but it does not colocalize with the recycling endosome-marker transferrin (Figure 3.7). Considering that the incubation time with the anti-HA antibody was two hours, these findings are consistent with our previous conclusions that kAE1 G701D is internalized from the cell surface within an hour (Figure 3.6) and that 50% of kAE1 G701D is degraded 4 hours after its biosynthesis (Figure 3.1). No colocalization was found between Lamp-1 and kAE1 WT (Figure 3.7), in agreement with the longer half-life of kAE1 WT protein (Figure 3.1). These findings confirmed the implication of the lysosomal pathway for the degradation of kAE1 G701D after its internalization from the cell surface.

4.4 Leupeptin treatment can improve the function of kAE1 G701D

In our previous paper, we showed that a 16 hours treatment with 1% DMSO can partially rescue trafficking and function of the dRTA Golgi retained kAE1 G701D mutant to the cell surface of MDCK cells (Chu, King et al. 2013). However, we have not been able to completely rescue the functionality of this mutant. We found that its short half-life, compared to that of kAE1 WT protein, explains the gap between the functional activity level of kAE1 WT and that of kAE1 G701D (Chu, King et al. 2013). Indeed, inhibiting kAE1 G701D premature degradation restores its activity to a level comparable to kAE1 WT protein (figure 3.9).

The leupeptin-mediated stabilization of kAE1 G701D improved the functional activity of this mutant to a level that is not significantly different to the WT protein (Figure 3.9). The improvement due to the leupeptin treatment was more evident when the cells were treated only with leupeptin rather than when they were treated with leupeptin and DMSO together (Figure 3.9). This could eventually suggest that the presence of leupeptin affects the rescuing action of DMSO or vice versa. To elucidate this point we should have performed an experiment to verify the effect of DMSO on leupeptin's action. For instance, we could have used a control protein, ubiquitously expressed in mammalian cells and known to be degraded by lysosomes, such as HMG-CoA reductase (Tanaka, Li et al. 1986), and we could verify if leupeptin-mediated stabilization of this protein is affected or not by the presence of DMSO. These functional data have to be interpreted carefully, as the functional assays we performed did not measure directly the activity of the kAE1 protein. Our functional assay uses variations of BCECF emitted fluorescence that reflect the effect kAE1 has on intracellular pH as discussed in the Materials and Methods section. As the kAE1 imports bicarbonate molecules, it relies on endogenous carbonic anhydrase II activity to alter intracellular pH. It is thus possible that leupeptin or DMSO treatments have

an undesirable effect on carbonic anhydrase II activity or stability. Thus, the limitation of this technique is represented by the fact that we do not measure directly the activity of the protein but just a secondary effect of its activity. More reliable data could have been obtained by a direct measurement of kAE1-mediated efflux of radioactive isotopes such as Cl^- or SO_4^{2-} , which is also a substrate of kAE1 (Funder et al. 1976).

4.5 Knocking down the peripheral quality control machinery helps to stabilize kAE1 G701D

In our work, we also showed that knocking-down the Hepatocyte growth factor-regulated (Hrs) and the Signal Transducing Adaptor Protein (STAM) component of the peripheral quality control machinery led to a stabilization of the total amount of kAE1 G701D (Figure 3.8). Although DMSO incubation partially rescued the function of kAE1 G701D, the mutant is endocytosed and recognized by the peripheral quality control machinery that targets it for degradation. Our findings indicate that the two components Hrs and STAM are critical for the targeting of the endocytosed kAE1 G701D to the lysosome. Knocking-down of Tumor susceptibility gene 101 (Tsg101), instead, had no significant effect on the total amount of kAE1 G701D, thus suggesting a correct activity of the quality-control machinery even in absence of this component. Although we did not control for the extent of the knock-down for each component of the quality-control machinery, we relied on published data to perform the knockdown experiments (Bache, Stuffers et al. 2006). Furthermore we have to consider as well that HeLa cells are not kidney cells. We used HeLa cells since it is relatively easy to knock-down endogenous proteins in these cells, and because these cells were available from Dr. Gergely Lukacs's laboratory (McGill University). Since we were conducting a research about kAE1, it would have been ideal to use kidney cells like MDCK cells.

Finally, in this study we considered just a limited number of components of the peripheral quality control machinery (Okiyoneda, Barriere et al. 2010) and to acquire a better knowledge of the degradation machinery involved in this process, it would be necessary to knock-down every component to understand which are the most critical ones.

4.6 Ndfip1 interacts with kAE1 G701D

As shown in Figure 3.4, kAE1 mutants are poly-ubiquitylated. We focused on Nedd4 family interacting protein 1 (Ndfip1) because it is an adaptor of the ubiquitin ligase Nedd4, the enzyme that causes ubiquitin attachment on the target protein. Therefore, this protein is involved in the ubiquitylation process (Goh, Low et al. 2013). Goh et al. showed that, in yeast, Ndfip1 is located in the Golgi, where it detects polar residues within transmembrane domains (Goh, Low et al. 2013). As kAE1 G701D introduces a polar residue in the ninth transmembrane domain of kAE1, we hypothesized that Ndfip1 interacts with kAE1 G701D mutant and promotes its poly-ubiquitylation and premature degradation. We obtained Ndfip1 cDNA from Dr. Kumar Sharad (Centre for Cancer Biology, Adelaide, Australia) and we over-expressed it in MDCK cells expressing kAE1 WT or G701D mutant. Our immunoprecipitation assay showed an interaction between Ndfip1 and kAE1 G701D and confirmed our hypothesis, suggesting that Ndfip1 may be involved in the ubiquitylation process of kAE1 G701D. Interestingly, the blots show very faint kAE1 WT band with complex oligosaccharides when co-expressed with Ndfip1, suggesting that in this condition just a small amount of WT protein can be properly targeted to the cell surface (Figure 3.11). This observation is consistent with the immunofluorescence results (Figure 3.10) showing less staining of kAE1 WT at the cell surface when it is co-expressed with Ndfip1 compared to when co-expressed with the empty vector pcDNA3. Of note, we noticed that, despite the fact that Ndfip1 transfection is easier in LLC-PK1 cells than in MDCK cells, the transfection efficiency we obtained was less than 50 % (Figure X). Remarkably, Harvey et al. showed that

overexpression of Ndfip1 results in cytotoxic effect by disrupting Golgi membranes and affecting Golgi normal function (Harvey et al. 2001). This fact could explain why kAE1 WT trafficking to the cell surface is affected when the protein is co-expressed with Ndfip1. Unfortunately, due to the lack of time, we have not been able to test our hypothesis that Ndfip1 is involved in kAE1 ubiquitylation process.

4.7 Final remarks

In this research, we have shown a way to improve kAE1 G701D mutant stability at the cell surface and to rescue its functional activity. Further, we provided new insights into the cellular mechanisms that degrade a non-native Golgi-retained mutant protein, showing the role of the lysosomal degradation pathway and the involvement of the ESCRT. Also, we demonstrated that Ndfip1 interacts with kAE1 and especially with kAE1 G701D mutant, suggesting that Ndfip1 may be involved in its degradation. Since we know Ndfip1 specifically interacts with polar residues within transmembrane domains of proteins (Goh, Low et al. 2013), future experiments will be designed to investigate possible interactions between this molecule and the artificial mutant kAE1 G701A that lacks the polar aspartate residue present in kAE1 G701D mutant (Cordat et al., Traffic 2006). To complete our understanding of the effect of Ndfip1 on Golgi quality control machinery, experiments performed on an Ndfip1 – knocked down cell line might provide useful information about how Ndfip1 affects kAE1 G701D ubiquitylation levels, its stability at the cell surface and its functional activity.

Nevertheless, many aspects of these degradation mechanisms remain unclear. For instance, the information we provided about the importance of some peripheral quality control machinery components is incomplete and will require further investigations, ideally performed on kidney cells.

Beside dRTA, other diseases caused by a Golgi-retained mutant protein have been described: the E258K mutation of aquaporin-2, for instance, is retained

in the Golgi, thus resulting in nephrogenic diabetes insipidus (Mulders et al. 1998). Further elucidation of the degradation mechanisms that involve Golgi-retained mutants might unveil novel targets for restoring protein functional activity, and provide new therapeutic strategies for patients with these mutations.

Bibliography

Bibliography

Aebi, M. (2013). "N-linked protein glycosylation in the ER." Biochim Biophys Acta **1833**(11): 2430-2437.

Al-Awqati, Q. and X. B. Gao (2011). "Differentiation of intercalated cells in the kidney." Physiology (Bethesda) **26**(4): 266-272.

Almomani, E, J. C. King, J. Netsawang, P. T. Yenchitsomanus, P. Malasit, T. Limjindaporn, R. T. Alexander and E. Cordat (2012). "Adaptor protein 1 complexes regulate intracellular trafficking of the kidney anion exchanger 1 in epithelial cells." Am J Physiol Cell Physiol **303**(5): C554-566.

Bache, K. G., Stuffers, S., Lukacs G. L., Stenmark, "The ESCRT-III subunit hVps24 is required for degradation but not silencing of the epidermal growth factor receptor." Mol Biol Cell. 2006 Jun;17(6):2513-23.

Bagnis, C., V. Marshansky, S. Breton and D. Brown (2001). "Remodeling the cellular profile of collecting ducts by chronic carbonic anhydrase inhibition." Am J Physiol Renal Physiol **280**(3): F437-448.

Barcellini, P. Bianchi, E. Fermo, F. G. Imperiali, A. P. Marcello, C. Vercellati, A. Zaninoni and A. Zanella (2011). "Hereditary red cell membrane defects: diagnostic and clinical aspects." Blood Transfus **9**(3): 274-277.

Barneaud-Rocca, D., C. Etchebest. Guizouarn (2013). "Structural model of the anion exchanger 1 (SLC4A1) and identification of transmembrane segments forming the transport site." J Biol Chem **288**(37): 26372-26384.

Basu, A., S. Mazor and J. R. Casey (2010). "Distance measurements within a concatamer of the plasma membrane Cl(-)/HCO(3)(-) exchanger, AE1." Biochemistry **49**(43): 9226-9240.

Battle, D. and S. K. Haque (2012). "Genetic causes and mechanisms of distal renal tubular acidosis." Nephrol Dial Transplant **27**(10): 3691-3704.

Benham, A. M. (2012). "Protein secretion and the endoplasmic reticulum." Cold Spring Harb Perspect Biol **4**(8): a012872.

Blumer, J., J. Rey, L. Dehmelt, T. Mazel, Wu, P. Bastiaens, R. S. Goody and A. Itzen (2013). "RabGEFs are a major determinant for specific Rab membrane targeting." J Cell Biol **200**(3): 287-300.

Bohdanowicz, M. and S. Grinstein (2013). "Role of phospholipids in endocytosis, phagocytosis, and macropinocytosis." Physiol Rev **93**(1): 69-106.

Bonar, P., Casey, J. R. (2008) "Plasma membrane $\text{Cl}^-/\text{HCO}_3^-$ exchangers. Structure, mechanism and physiology." Landes Bioscience 337-345

Bruce, L. J., D. L. Cope, G. K. Jones, A. E. Schofield, M. Burley, S. Povey, R. J. Unwin, O. Wrong and M. J. Tanner (1997). "Familial distal renal tubular acidosis is associated with mutations in the red cell anion exchanger (Band 3, AE1) gene." J Clin Invest **100**(7): 1693-1707.

Bruce, L. J., O. Wrong, A. M. Toye, M. T. Young, G. Ogle, Z. Ismail, A. K. Sinha, P. McMaster, I. Hwaihwanje, G. B. Nash, S. Hart, E. Lavu, R. Palmer, A. Othman, R. J. Unwin and M. J. Tanner (2000). "Band 3 mutations, renal tubular acidosis and South-East Asian ovalocytosis in Malaysia and Papua New Guinea: loss of up to 95% band 3 transport in red cells." Biochem J **350 Pt 1**: 41-51.

Butler, G. S. and C. M. Overall (2009). "Proteomic identification of multitasking proteins in unexpected locations complicates drug targeting." Nat Rev Drug Discov **8**(12): 935-948.

Casey, J. R. and R. A. Reithmeier (1998). "Anion exchangers in the red cell and beyond." Biochem Cell Biol **76**(5): 709-713.

Chang, H. H., C. F. Shaw, S. H. Jian, K. H. Hsieh, H. H. Chiou and P. J. Lu (2009). "Compound mutations in human anion exchanger 1 are associated with complete distal renal tubular acidosis and hereditary spherocytosis." Kidney Int **76**(7): 774-783.

Cheung, J. C., J. Li and R. A. Reithmeier (2005). "Topology of transmembrane segments 1-4 in the human chloride/bicarbonate anion exchanger 1 (AE1) by scanning N-glycosylation mutagenesis." Biochem J **390**(Pt 1): 137-144.

Chu, C. H., J. C. King, M. Berrini, R. T. Alexander and E. Cordat (2013). "Functional rescue of a kidney anion exchanger 1 trafficking mutant in renal epithelial cells." PLoS One **8**(2): e57062.

Clague, M. J. and S. Urbe (2010). "Ubiquitin: same molecule, different degradation pathways." Cell **143**(5): 682-685.

Conn, P. M., A. Ulloa-Aguirre, J. Ito and J. A. Janovick (2007). "G protein-coupled receptor trafficking in health and disease: lessons learned to prepare for therapeutic mutant rescue in vivo." Pharmacol Rev **59**(3): 225-250.

Cordat, E. (2006). "Unraveling trafficking of the kidney anion exchanger 1 in polarized MDCK epithelial cells." Biochem Cell Biol **84**(6): 949-959.

Cortes, A., A. Benet, B. M. Cooke, J. H. Barnwell and J. C. Reeder (2004). "Ability of Plasmodium falciparum to invade Southeast Asian ovalocytes varies between parasite lines." Blood **104**(9): 2961-2966.

Duangtum, N., M. Junking, N. Sawasdee, B. Cheunschon, T. Limjindaporn and P. T. Yenchitsomanus (2011). "Human kidney anion exchanger 1 interacts with kinesin family member 3B (KIF3B)." Biochem Biophys Res Commun **413**(1): 69-74.

Fan, C., Wang, W., Zhao, B., Zhang, S., Miao, J. (2006) "Chloroquine inhibits cell growth and induces cell death in A549 lung cancer cells." Bioorg Med Chem. 3218-22

Fry, A. C. and F. E. Karet (2007). "Inherited renal acidoses." Physiology (Bethesda) **22**: 202-211.

Fry, A. C., H. Su, V. Yiu, A. H. Cuthbert, H. Trachtman and F. E. Karet Frankl (2012). "Mutation conferring apical-targeting motif on AE1 exchanger causes autosomal dominant distal RTA." J Am Soc Nephrol **23**(7): 1238-1249.

Funder, J., Wieth, J. O. (1976) "Chloride transport in human eryt

Glodny, B., V. Unterholzner, B. Taferner, K. J. Hofmann, P. Rehder, A. Strasak and J. Petersen (2009). "Normal kidney size and its influencing factors - a 64-slice MDCT study of 1.040 asymptomatic patients." BMC Urol **9**: 19.

Goh, C. P., L. H. Low, U. Putz, J. Gunnensen, V. Hammond, J. Howitt and S. S. Tan (2013). "Ndfip1 expression in developing neurons indicates a role for protein ubiquitination by Nedd4 E3 ligases during cortical development." Neurosci Lett **555**: 225-230.

Golembiewska, E. and K. Ciechanowski (2012). "Renal tubular acidosis--underrated problem?" Acta Biochim Pol **59**(2): 213-217.

Henley, J. R., H. Cao and M. A. McNiven (1999). "Participation of dynamin in the biogenesis of cytoplasmic vesicles." FASEB J **13 Suppl 2**: S243-247.

Hinson, D. L., Webber, R. J. (1988) "Miniaturization of the protein BCA assay." Biotechniques. 1988 Jan;6(1):14, 16, 19.

Hou, J., M. Rajagopal and A. S. Yu (2013). "Claudins and the kidney." Annu Rev Physiol **75**: 479-501.

Hsu, V. , S. . Lee and J. S. Yang (2009). "The evolving understanding of COPI vesicle formation." Nat Rev Mol Cell Biol **10**(5): 360-364.

Huber, S., E. Asan, T. Jons, C. Kerscher, B. Puschel and D. Drenckhahn (1999). "Expression of rat kidney anion exchanger 1 in type A intercalated cells in metabolic acidosis and alkalosis." Am J Physiol **277**(6 Pt 2): F841-849.

Hung, M. C. and . Link (2011). "Protein localization in disease and therapy." J Cell Sci **124**(Pt 20): 3381-3392.

Huotari, J. and A. Helenius (2011). "Endosome maturation." EMBO J **30**(17): 3481-3500.

Jung, T. and T. Grune (2013). "The proteasome and the degradation of oxidized proteins: Part I-structure of proteasomes." Redox Biol **1**(1): 178-182.

Keskanokwong, T., J. Shandro, D. E. Johnson, S. Kittanakom, G. L. Vilas, P. Thorner, R. A. Reithmeier, V. Akkarapatumwong, P. T. Yenchitsomanus and J. R. Casey (2007). "Interaction of integrin-linked kinase with the kidney chloride/bicarbonate exchanger, kAE1." J Biol Chem **282**(32): 23205-23218.

Kittanakom, S., E. Cordat and R. A. Reithmeier (2008). "Dominant-negative effect of Southeast Asian ovalocytosis anion exchanger 1 in compound heterozygous distal renal tubular acidosis." Biochem J **410**(2): 271-281.

Kleiger, G. and T. Mayor (2014). "Perilous journey: a tour of the ubiquitin-proteasome system." Trends Cell Biol.

Kumar, S., K. F. Harvey, M. Kinoshita, N. G. Copeland, M. Noda and N. A. Jenkins (1997). "cDNA cloning, expression analysis, and mapping of the mouse Nedd4 gene." Genomics **40**(3): 435-443.

Le Saux, O., K. Fulop, Yamaguchi, A. Ilias, Z. Szabo, C. N. Brampton, V. Pomozi, K. Huszar, T. Aranyi and A. Varadi (2011). "Expression and in vivo

rescue of human ABCC6 disease-causing mutants in mouse liver." PLoS One **6**(9): e24738.

Liu, J., Lu, D. Reigada, J. Nguyen, A. M. Laties and C. Mitchell (2008). "Restoration of lysosomal pH in RPE cells from cultured human and ABCA4(-/-) mice: pharmacologic approaches and functional recovery." Invest Ophthalmol Vis Sci **49**(2): 772-780.

Loo, T. , M. C. Bartlett and D. M. Clarke (2013). "Corrector VX-809 stabilizes the first transmembrane domain of CFTR." Biochem Pharmacol **86**(5): 612-619.

Mohandas, N., L. E. Lie-Injo, M. Friedman and J. Mak (1984). "Rigid membranes of Malayan ovalocytes: a likely genetic barrier against malaria." Blood **63**(6): 1385-1392.

Norgett, E. E., Z. J. Golder, B. Lorente-Canovas, N. Ingham, K. P. Steel and F. E. Karet Frankl (2012). "Atp6v0a4 knockout mouse is a model of distal renal tubular acidosis with hearing loss, with additional extrarenal phenotype." Proc Natl Acad Sci U S A **109**(34): 13775-13780.

Okiyoneda, T., Barriere, M. Bagdany, M. Rabeh, K. Du, J. Hohfeld, J. C. Young and G. L. Lukacs (2010). "Peripheral protein quality control removes unfolded CFTR from the plasma membrane." Science **329**(5993): 805-810.

Pang, A. J., S. P. Bustos and R. A. Reithmeier (2008). "Structural characterization of the cytosolic domain of kidney chloride/bicarbonate anion exchanger 1 (kAE1)." Biochemistry **47**(15): 4510-4517.

Patterson, S. T., Reithmeier, R. A. (2010) "Cell surface rescue of kidney anion exchanger 1 mutants by disruption of chaperone interactions." J Biol Chem **285**(43):33432-34

Popov, M. and R. A. Reithmeier (1999). "Calnexin interaction with N-glycosylation mutants of a polytopic membrane glycoprotein, the human erythrocyte anion exchanger 1 (band 3)." J Biol Chem **274**(25): 17635-17642.

Rafferty, S., N. Alcolado, C. Norez, F. Chappe, S. Pelzer, F. Becq and V. Chappe (2009). "Rescue of functional F508del cystic fibrosis transmembrane conductance regulator by vasoactive intestinal peptide in the human nasal epithelial cell line JME/CF15." J Pharmacol Exp Ther **331**(1): 2-13.

Rosanas-Urgell, A., E. Lin, L. Manning, P. Rarau, M. Laman, N. Senn, B. T. Grimberg, L. Tavul, D. I. Stanisic, L. J. Robinson, J. J. Aponte, E. Dabod, J. C. Reeder, P. Siba, P. A. Zimmerman, T. M. Davis, C. L. King, P. Michon and I. Mueller (2012). "Reduced risk of *Plasmodium vivax* malaria in Papua New Guinean children with Southeast Asian ovalocytosis in two cohorts and a case-control study." PLoS Med **9**(9): e1001305.

Royle, S. J. (2006). "The cellular functions of clathrin." Cell Mol Life Sci **63**(16): 1823-1832.

Salhany, J. M. (2001). "Mechanistic basis for site-site interactions in inhibitor and substrate binding to band 3 (AE1): evidence distinguishing allosteric from electrostatic effects." Blood Cells Mol Dis **27**(5): 901-912.

Scheffner, M., U. Nuber and J. M. Huibregtse (1995). "Protein ubiquitination involving an E1-E2-E3 enzyme ubiquitin thioester cascade." Nature **373**(6509): 81-83.

Schreuder, M. F. (2012). "Safety in glomerular numbers." Pediatr Nephrol **27**(10): 1881-1887.

Shao, S. and R. S. Hegde (2011). "Membrane protein insertion at the endoplasmic reticulum." Annu Rev Cell Dev Biol **27**: 25-56.

Shibata, S., J. Rinehart, J. Zhang, G. Moeckel, M. Castaneda-Bueno, A. L. Stiegler, T. J. Boggon, G. Gamba and R. P. Lifton (2013). "Mineralocorticoid receptor phosphorylation regulates ligand binding and renal response to volume depletion and hyperkalemia." Cell Metab **18**(5): 660-671.

Stehberger, P. A., B. E. Shmukler, A. K. Stuart-Tilley, L. L. Peters, S. L. Alper and C. A. Wagner (2007). "Distal renal tubular acidosis in mice lacking the AE1 (band3) Cl⁻/HCO₃⁻ exchanger (slc4a1)." J Am Soc Nephrol **18**(5): 1408-1418.

Stenmark, H. and V. M. Olkkonen (2001). "The Rab GTPase family." Genome Biol **2**(5): REVIEWS3007.

Sterling, D., B. V. Alvarez and J. R. Casey (2002). "The extracellular component of a transport metabolon. Extracellular loop 4 of the human AE1 Cl⁻/HCO₃⁻ exchanger binds carbonic anhydrase IV." J Biol Chem **277**(28): 25239-25246.

Su, H., K. G. Blake-Palmer, A. C. Fry, A. Best, A. C. Brown, T. F. Hiemstra, S. Horita, A. Zhou, A. M. Toye and F. E. Karet (2011). "Glyceraldehyde 3-phosphate dehydrogenase is required for band 3 (anion exchanger 1) membrane residency in the mammalian kidney." Am J Physiol Renal Physiol **300**(1): F157-166.

Tanaka, R. D., Li, A. C., Fogelman, A. M., Edwards, P. A. (1986). "Inhibition of lysosomal protein degradation inhibits the basal degradation of 3-hydroxy-3-methylglutaryl coenzyme A reductase" J Lipid Res, 1986. 27: 261-273.

Toye, A. M., G. Banting and M. J. Tanner (2004). "Regions of human kidney anion exchanger 1 (kAE1) required for basolateral targeting of kAE1 in polarised kidney cells: mis-targeting explains dominant renal tubular acidosis (dRTA)." J Cell Sci **117**(Pt 8): 1399-1410.

Ungsupravate, D., N. Sawasdee, S. Khositseth, H. Udomchaiprasertkul, S. Khoprasert, J. Li, R. A. Reithmeier and P. T. Yenchitsomanus (2010). "Impaired trafficking and intracellular retention of mutant kidney anion exchanger 1 proteins (G701D and A858D) associated with distal renal tubular acidosis." Mol Membr Biol **27**(2-3): 92-103.

Unwin, R. J., D. G. Shirley and G. Capasso (2002). "Urinary acidification and distal renal tubular acidosis." J Nephrol **15 Suppl 5**: S142-150.

van Meel, E. and J. Klumperman (2008). "Imaging and imagination: understanding the endo-lysosomal system." Histochem Cell Biol **129**(3): 253-266.

Vasuvattakul, S. (2010). "Molecular Approach for Distal Renal Tubular Acidosis Associated AE1 Mutations." Electrolyte Blood Press **8**(1): 25-31.

Vijayakumar, S., J. Takito, C. Hikita and Q. Al-Awqati (1999). "Hensin remodels the apical cytoskeleton and induces columnarization of intercalated epithelial cells: processes that resemble terminal differentiation." J Cell Biol **144**(5): 1057-1067.

Wagner, C. A., O. Devuyst, S. Bourgeois and N. Mohebbi (2009). "Regulated acid-base transport in the collecting duct." Pflugers Arch **458**(1): 137-156.

Walder, J. A., R. Chatterjee, T. L. Steck, P. S. Low, G. F. Musso, E. T. Kaiser, P. Rogers and A. Arnone (1984). "The interaction of hemoglobin with the

cytoplasmic domain of band 3 of the human erythrocyte membrane." J Biol Chem **259**(16): 10238-10246.

Wall, S. M. (2005). "Recent advances in our understanding of intercalated cells." Curr Opin Nephrol Hypertens **14**(5): 480-484.

Wang, . B., V. Leroy, A. B. Maunsbach, A. Doucet, U. Hasler, E. Dizin, T. Hernandez, S. de Seigneux, P. . Martin and E. Feraille (2014). "Sodium Transport Is Modulated by p38 Kinase-Dependent Cross-Talk between ENaC and Na,K-ATPase in Collecting Duct Principal Cells." J Am Soc Nephrol **25**(2): 250-259.

Williamson, R. C., A. C. Brown, H. J. Mawby and A. M. Toye (2008). "Human kidney anion exchanger 1 localisation in MDCK cells is controlled by the phosphorylation status of two critical tyrosines." J Cell Sci **121**(Pt 20): 3422-3432.

Wrong, O., L. J. Bruce, R. J. Unwin, A. M. Toye and M. J. Tanner (2002). "Band 3 mutations, distal renal tubular acidosis, and Southeast Asian ovalocytosis." Kidney Int **62**(1): 10-19.

Wu, F., M. A. Saleem, N. B. Kampik, T. J. Satchwell, R. C. Williamson, S. M. Blattner, L. Ni, T. Toth, G. White, M. T. Young, M. D. Parker, S. L. Alper, C. A. Wagner and A. M. Toye (2010). "Anion exchanger 1 interacts with nephrin in podocytes." J Am Soc Nephrol **21**(9): 1456-1467.

Wu, F., T. J. Satchwell and A. M. Toye (2011). "Anion exchanger 1 in red blood cells and kidney: Band 3's in a pod." Biochem Cell Biol **89**(2): 106-114.

Yenchitsomanus, P. T., S. Kittanakom, N. Rungroj, E. Cordat and R. A. Reithmeier (2005). "Molecular mechanisms of autosomal dominant and recessive distal renal tubular acidosis caused by SLC4A1 (AE1) mutations." J Mol Genet Med **1**(2): 49-62.

Zhang, Z., K. X. Liu, J. He, Z. Fu, Yue, Zhang, C. Q. Zhang and Z. L. Zhang (2012). "Identification of two novel mutations in the SLC4A1 gene in two unrelated Chinese families with distal renal tubular acidosis." Arch Med Res **43**(4): 298-304.